Microbial Ecology (2018) 76:866–884
https://doi.org/10.1007/s00248-018-1179-z

MICROBIOLOGY OF AQUATIC SYSTEMS

# Vertical and Seasonal Patterns Control Bacterioplankton Communities at Two Horizontally Coherent Coastal Upwelling Sites off Galicia (NW Spain)

Víctor Hernando-Morales[1,2] · Marta M. Varela[3] · David M. Needham[4] · Jacob Cram[4,5] · Jed A. Fuhrman[4] · Eva Teira[1,2]

Received: 5 March 2017 / Accepted: 14 March 2018 / Published online: 19 April 2018


## Abstract

Analysis of seasonal patterns of marine bacterial community structure along horizontal and vertical spatial scales can help to predict long-term responses to climate change. Several recent studies have shown predictable seasonal reoccurrence of bacterial assemblages. However, only a few have assessed temporal variability over both horizontal and vertical spatial scales. Here, we simultaneously studied the bacterial community structure at two different locations and depths in shelf waters of a coastal upwelling system during an annual cycle. The most noticeable biogeographic patterns observed were seasonality, horizontal homogeneity, and spatial synchrony in bacterial diversity and community structure related with regional upwelling–downwelling dynamics. Water column mixing eventually disrupted bacterial community structure vertical heterogeneity. Our results are consistent with previous temporal studies of marine bacterioplankton in other temperate regions and also suggest a marked influence of regional factors on the bacterial communities inhabiting this coastal upwelling system. Bacterial-mediated carbon fluxes in this productive region appear to be mainly controlled by community structure dynamics in surface waters, and local environmental factors at the base of the euphotic zone.

**Keywords** Bacterioplankton community · Spatial and temporal variability · Spatial synchrony · Upwelling-downwelling · ARISA

## Introduction

Marine bacterioplankton communities are dynamic and patchily distributed, showing variation over different spatial and temporal scales. Previous studies have shown moderate changes of the bacterial communities over large horizontal scales [13, 81, 94, 95, 104]. In fact, processes influencing bacterial community structure (BCS) over horizontal spatial scales have been suggested to be heterogeneous at scales > 50 km in the open ocean [63]. Variation along vertical scales appears to be comparatively more marked [1, 77, 81]. Nevertheless, the variability of bacterial communities over spatial scales may be strongly affected by dispersal-related filters and hydrographic processes in the ocean, separating or mixing water masses at different temporal scales [62].

Irrespective of spatial variability, several studies have shown temporal dynamics of marine bacterial communities over a wide range of timescales, ranging from diel to interannual fluctuations [11, 23, 28, 54, 55, 73, 80, 82, 34, 3]. Some of these temporal fluctuations occur at short scales (days) [63, 82, 83, 84, 111, 112], but short-term changes tend to oscillate about a predisturbed community over weeks yielding stability over the scale of weeks to months, suggesting a strong ecological resilience regulated by longer term factors [47, 82, 103].

**Electronic supplementary material** The online version of this article (https://doi.org/10.1007/s00248-018-1179-z) contains supplementary material, which is available to authorized users.

✉ Víctor Hernando-Morales
vhernando@uvigo.es

1 Grupo de Oceanografía Biolóxica, Departamento de Ecoloxía e Bioloxía Animal, Universidade de Vigo, 36310 Vigo, Spain

2 Estación de Ciencias Mariñas de Toralla (ECIMAT), Universidade de Vigo, Illa de Toralla, 36331 Vigo, Spain

3 IEO, Instituto Español de Oceanografía, Centro Oceanográfico de A Coruña, Apdo 130, 15080 A Coruña, Spain

4 Department of Biological Sciences, University of Southern California, Los Angeles, CA 90089-0371, USA

5 School of Oceanography, University of Washington, Seattle, WA 98195, USA

Even though the study of bacterioplankton communities along the three different dimensions (i.e., horizontal space, depth, and time) is critical to understand, model, and eventually predict distribution patterns in the oceans [46], only a few biogeographic studies have assessed variability over both spatial and seasonal scales [1, 42, 51, 53, 63]. To capture spatial and temporal diversity patterns in coastal areas (excluding strong physicochemical spatial gradients such as estuary-coast transition), sampling must occur at horizontal scales ranging from tens to hundreds of kilometers, at vertical scales enabling comparison of different ecological niches, and at the order of weekly to monthly timescales over, at least, an annual cycle. Owing to the lack of such studies, our current understanding of the extent and predictability of microbial diversity patterns is still limited, and only broad interpretations from worldwide comparisons of long-term time series are emerging [47, 56].

Temporal and spatial differences in phytoplankton communities have been extensively reported along the Galician coast related to both upwelling–downwelling patterns and the Finisterre Front [17, 18, 24, 39, 109, 115]. Such differences in phytoplankton dynamics, together with the short-term and seasonal changes in meteorological conditions (e.g., solar radiation, precipitation), may drive changes in the carbon fluxes through the microbial communities along the seasonal cycle, and thus affect the structure and function of the bacterial community [109].

Compared to other microbial plankton components, very few studies have described bacterioplankton dynamics in this highly productive ecosystem [79, 109, 114]. The few attempts to describe bacterial diversity have been limited to the inner part of the Ría de Vigo [2, 110, 119].

Within this context, the objective of our work was to simultaneously study the bacterioplankton community structure at two depths in shelf waters off the Rías Altas (in front of A Coruña) and off the Rías Baixas (in front of Ría de Vigo) during an annual cycle using ARISA fingerprinting in order to (1) describe the spatial and temporal BCS variability, (2) to identify which factors drive bacterial biogeographic patterns in this coastal region, and (3) to relate environmental variability, BCS, and bacterial-mediated carbon fluxes.

We hypothesized that euphotic zone bacterial communities would show clear seasonal patterns and significantly differ between both sampling locations and depths.

## Material and Methods

### Study Area

The coastal area off Galicia represents the northern boundary of the Eastern North Atlantic upwelling system [6, 14, 25]. Northerly winds, which favor upwelling, occur in the region from spring (March–April) until fall (September–October), and southerly winds favoring downwelling predominate the rest of the year (October to March) [6, 25, 118]. A subsurface front develops off Cape Finisterre during the upwelling period [7, 27, 43, 44, 61, 76] where two varieties of Eastern North Atlantic Central Water (ENACW) converge: relatively warm (> 13 °C) ENACW of subtropical origin ($ENACW_{st}$) and the colder (< 13 °C) nutrient-richer ENACW of subpolar origin ($ENACW_{sp}$). $ENACW_{st}$ preferentially upwells in the large coastal embayments located to the south of Cape Finisterre, coined as "Rías Baixas" [5], whereas $ENACW_{sp}$ preferentially upwells in the "Rías Altas" located to the north of Cape Finisterre (Fig. 1) [6, 25, 41, 90, 96]. This coastal area has a mild climate in comparison to similar latitudes on the other side of the Atlantic. The inter-annual variation in seasonal dynamics falls between temperate and oceanic climates, generally features tempered summers (relative to their latitude) and exceptionally mild winters, consistently heavy rainfall, and temperatures rarely dropping below freezing. We will use hereafter the term "seasonal" for those variables showing strong and significant correlation with day length (D-L), even though our dataset only covers a single annual cycle.

### Meteorological and Hydrographic Variables

Precipitation (PPT) and D-L data were obtained from two meteorological stations close to the sampling points (*A Coruña Dique Station* and *Islas Cíes Station* for A Coruña

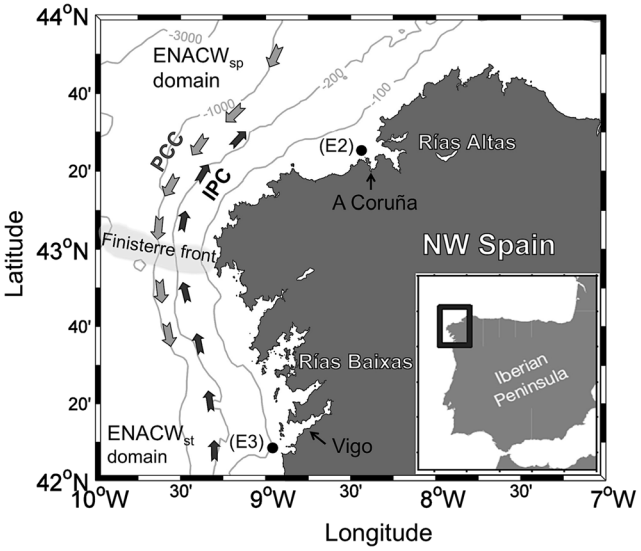


**Fig. 1** Galician coast map (NW coast of the Iberian Peninsula) showing sampling locations off A Coruña (E2) and Vigo (E3), bathymetry, and main components of the Eastern North Atlantic Central Water (ENACW) water mass boundaries (sp, subpolar; st, subtropical) and the Portugal Coastal Current (PCC) systems. Black dots indicate stations where bacterial community structure was sampled monthly. Gray arrows indicate main current of the PCC, and black arrows indicate main current of the Iberian Poleward Current (IPC)

and Vigo datasets, respectively). The upwelling intensity was estimated as an upwelling index (Iw) by calculating the Ekman transport from surface winds. Daily Iw values were computed in two cells of 1° × 1° centered at 43.5° N, 9° W for A Coruña and at 42° N, 10° W for Vigo, by the Instituto Español de Oceanografía (http://www.indicedeafloramiento.ieo.es/) [58], using data from atmospheric pressure at sea level derived from the WXMAP model [Bode, pers. comm.]. The upper mixed layer (UML) depth was determined as the depth where temperature differed by more than 0.25 °C the surface value.

## Sampling

Seawater samples were collected at two shelf stations off the Galician coast, northwest Spain [A Coruña (E2) Vigo (E3), see Fig. 1] over an annual cycle at approximately monthly intervals (January to December 2010). In November 2010, E3 could not be sampled because of stormy weather.

At each sampling date, vertical profiles of temperature, salinity, chlorophyll-fluorescence, and photosynthetically active radiation (PAR) were obtained with a SBE-25 CTD equipped with a Seapoint in situ fluorometer and a Licor spherical PAR sensor. Water from seven fixed levels (surface, 5, 10, 20, 30–40 (A Coruña) / 50 (Vigo), and 70 (A Coruña) / 75 (Vigo) m) was sampled with 5-L Niskin bottles that were attached to a CTD rosette sampler (A Coruña) or to the hydrographic wire (Vigo). The bottom depths at E2 and E3 were 77 and 97 m, respectively. Inorganic nutrients (ammonium, nitrite, nitrate, phosphate, and silicate) and chlorophyll-*a* (Chl-*a*) concentrations were sampled at all depths. Inorganic nutrient concentration samples were collected in polyethylene bottles and frozen at − 20 °C until analysis by standard colorimetric methods with a Bran–Luebbe segmented flow analyzer. Chl-*a* concentration was determined from acetonic extracts of plankton retained by GF/F filters and measured by the fluorimetric method [88].

## Additional Contextual Variables

Total dissolved nitrogen (TDN), dissolved organic carbon (DOC) concentration, particulate organic carbon and nitrogen (POC and PON) concentrations, fluorescence of dissolved organic matter [protein-like substrates (FDOM*t*) and humic-like substrates (FDOM*m*)], particulate and dissolved primary production (POCp and DOCp), bacterial respiration (BR), bacterial biomass (BB), and bacterial production (BP) were determined only at two depths (Table 1), corresponding approximately to the optical depths of 100% (surface) and 1% (corresponding to a variable depth ranging from 30 to 40 in A Coruña and to 50 m in Vigo) of surface PAR ($E_0$).

For DOC analysis, seawater was filtered through 0.2-μm filters (Pall, Supor membrane disc filter) and collected into precombusted (450 °C, 12 h) 10-mL glass ampoules in an all-glass filtration system under positive pressure of $N_2$, Ampoules were acidified with $H_3PO_4$ to pH < 2 and then heat sealed. DOC was subsequently measured in a Shimadzu TOC-V analyzer (Pt-catalyst). Fluorescence intensity was measured at the excitation/emission wavelengths of 320/410 nm (FDOM-M), characteristic of marine humic-like substances, and of 280/350 nm (FDOM-T), characteristic of protein-like materials [31]. POC and PON concentrations were determined in 0.5–1.0 L of seawater filtered through Whatman GF/F filters, which were stored frozen (− 20 °C) until analysis in a Carlo Erba CHNSO 1108 analyzer.

For POCp and DOCp determination, three light and two dark acid-washed Pyrex glass bottles (36 mL in volume) were filled and inoculated with radio-labeled sodium bicarbonate ([74,370 KBq (2–10 μCi)] of $NaH^{14}CO_3$). Then, bottles were incubated ashore for 2–3 h in an incubator which simulated surface seawater temperature and irradiance experienced by the cells at the original sampling depths. After incubation, two 5 mL subsamples were filtered through 0.2 μm polycarbonate filters. After removing inorganic $^{14}C$ by acidification, the radioactivity on filters and filtrates was determined with a β-scintillation counter to derive POCp and DOCp, respectively. The percentage of extracellular release (PER) was calculated by dividing DOCp by TOCp (POCp + DOCp) rates. For the estimation of BB, the abundance of heterotrophic bacteria was determined with a Becton Dickinson FACSCalibur flow cytometer equipped with a laser emitting at 488 nm [22]. Samples (1.8 mL) were preserved with 1% paraformaldehyde + 0.05% glutaraldehyde, and frozen at − 80 °C until analysis. Heterotrophic bacteria were stained with 2.5 mM SybrGreen DNA fluorochrome and identified on the basis of their fluorescence and light side scatter (SSC) signatures. Empirical calibrations between SSC and mean cell diameter described in Calvo-Díaz & Morán [22] were used to estimate biovolume of heterotrophic bacteria and finally converted into biomass by using the following allometric relationship of Norland [86]. BP was determined by the [$^3$H]-leucine incorporation method [64], modified as described by Smith and Azam [106]. Leucine was added to each sample (40 nM, final concentration) and incubated for 2 h in the same incubation chamber as the POC and DOC production bottles. Incubations were stopped by adding cold trichloroacetic acid (5%, final concentration). For comparative purposes, we used a theoretical leucine to carbon conversion of 3.1 kg C mol $Leu^{-1}$. BR was determined by the in vivo INT (2-para (iodophenyl)-3(nitrophenyl)-5(phenyl) tetrazolium chloride) reduction method [72]. Four 100-mL dark bottles were filled from each sampling depth, spiked with INT (final concentration 0.2 mM), and incubated in the same incubator chamber used for BP for 1–1.5 h. Formaldehyde-killed controls (2% *v*/*v* final concentration) were performed in order to account for any abiotic reduction of INT [72]. After incubation, samples

**Table 1** Mean (±SD) environmental and functional variables at the two sampling sites (A Coruña and Vigo) and the two optical depths [100 and 1% of surface photosynthetically active radiation ($E_0$)] during upwelling (Up) and downwelling (Dw) periods. Groups with no significant differences for a given variable (one-way ANOVA Kruskal–Wallis test) are indicated with the same letter

| Location | A Coruña | | | | Vigo | | | |
|---|---|---|---|---|---|---|---|---|
| PAR | 100% $E_0$ | | 1% $E_0$ | | 100% $E_0$ | | 1% $E_0$ | |
| Hydrographical situation | Up | Dw | Up | Dw | Up | Dw | Up | Dw |
| Environmental | | | | | | | | |
| Temperature (°C) | 15.1 ± 1.2a | 14.8 ± 1.7abc | 13.5 ± 0.5bc | 14.3 ± 1.2abc | 14.6 ± 1.4ab | 15.4 ± 2.3abc | 13.4 ± 0.6c | 14.3 ± 0.5a |
| Salinity | 35.3 ± 0.3d | 35.3 ± 0.4d | 35.7 ± 0.2ab | 35.7 ± 0.1bc | 35.1 ± 0.9cd | 34.4 ± 1.6d | 35.9 ± 0.1a | 35.8 ± 0.1a |
| PAR (μmol $m^{-2}$ $s^{-1}$) | 497 ± 295a | 228 ± 146ab | 7 ± 4c | 4 ± 5c | 433 ± 235a | 96 ± 67b | 2 ± 1c | 0.5 ± 0.3d |
| Silicate (μM) | 2.6 ± 1.7ab | 3.5 ± 1.8ab | 3.6 ± 1.4a | 3.5 ± 1.4a | 1.5 ± 0.7b | 3.3 ± 2.3ab | 3.9 ± 1.3a | 4.6 ± 1.4a |
| Phosphate (μM) | 0.3 ± 0.2ab | 0.3 ± 0.1a | 0.6 ± 0.3a | 0.4 ± 0.1a | 0.1 ± 0.1b | 0.2 ± 0.1ab | 0.4 ± 0.2a | 0.5 ± 0.2a |
| Nitrite (μM) | 0.2 ± 0.2a | 0.2 ± 0.2a | 0.3 ± 0.2a | 0.4 ± 0.3a | 0.4 ± 0.2a | 0.3 ± 0.3a | 0.3 ± 0.2a | 0.3 ± 0.2a |
| Nitrate (μM) | 2.3 ± 1.8b | 3.0 ± 1.8ab | 6.0 ± 2.9a | 4.0 ± 1.4a | 1.1 ± 0.9b | 2.9 ± 3.1ab | 7.2 ± 4.0a | 6.4 ± 3.3a |
| Ammonium (μM) | 1.5 ± 0.2a | 1.0 ± 0.23b | 1.1 ± 0.6abc | 0.7 ± 0.6bc | 2.1 ± 0.9a | 2.2 ± 1.8abc | 0.5 ± 0.3c | 0.8 ± 1.1abc |
| TDN (μM) | 18 ± 7abc | 18 ± 6ab | 11 ± 2c | 18 ± 8abc | 15 ± 2b | 19 ± 4ab | 21 ± 5a | 18 ± 7abc |
| DOC (μM) | 83 ± 14ab | 79 ± 7ab | 83 ± 16ab | 86 ± 9a | 75 ± 7ab | 78 ± 10ab | 70 ± 3b | 76 ± 4ab |
| POC (μM) | 14 ± 9ab | 8 ± 5bcde | 6 ± 2de | 4 ± 1e | 15 ± 3a | 11 ± 5abc | 6 ± 2cde | 10 ± 5abcd |
| PON (μM) | 1.6 ± 0.9ab | 1.1 ± 0.8abcd | 0.8 ± 0.3cd | 0.5 ± 0.1d | 2.1 ± 0.5a | 1.3 ± 0.7ab | 0.9 ± 0.4bc | 1.3 ± 0.7bc |
| FDOM*m* (ppb QS) | 3.0 ± 1.1b | 4.2 ± 3.1ab | 3.2 ± 2.5ab | 3.9 ± 2.2ab | 4.3 ± 2.3ab | 6.6 ± 4.1a | 3.8 ± 3.0ab | 3.2 ± 0.6b |
| FDOM*t* (ppb Trp) | 17 ± 13abc | 26 ± 8a | 17 ± 12abc | 20 ± 11abc | 8 ± 2bc | 10 ± 2b | 7 ± 2c | 10 ± 3bc |
| POCp (mg C $m^{-3}$$day^{-1}$) | 161 ± 140ab | 72 ± 96abcd | 29 ± 22cd | 5.8 ± 5.4de | 300 ± 226a | 40 ± 40bc | 2.5 ± 1.6e | 161 ± 140ab |
| PER (%) | 16 ± 11cd | 27 ± 24abcd | 25 ± 11bc | 43 ± 11a | 8 ± 7d | 11 ± 6d | 48 ± 20ab | 16 ± 11cd |
| Chl-*a* (mg $m^{-3}$) | 2.2 ± 2.4abc | 0.8 ± 0.8b | 1 ± 0.9abc | 0.3 ± 0.1c | 2.8 ± 1.7a | 1.0 ± 0.1ab | 0.2 ± 0.1c | 0.2 ± 0.0c |
| Functional | | | | | | | | |
| BB (mg C $m^{-3}$) | 8.8 ± 2.6a | 7.6 ± 6.7abc | 4.4 ± 1.4c | 4.5 ± 5.2bc | 15.6 ± 7.5a | 15.6 ± 12.5ab | 9.5 ± 9.6abc | 8.8 ± 2.6a |
| BP (mg C $m^{-3}$$day^{-1}$) | 17.5 ± 19.4ab | 2.7 ± 4.4b | 4.9 ± 6.0ab | 1.7 ± 1.8b | 12.3 ± 11.4a | 4.9 ± 3.1ab | 1.2 ± 0.4b | 17.5 ± 19.4ab |
| BR (mg C $m^{-3}$ $day^{-1}$) | 8.8 ± 7.3ab | 2.9 ± 2.1c | 3.3 ± 1.4bc | 2.7 ± 1.8c | 10.6 ± 7.8a | 11.9 ± 9.2ab | 2.6 ± 1.2c | 8.8 ± 7.3ab |

*PAR* photosynthetically active radiation, *TDN* total dissolved nitrogen, *DOC* dissolved organic carbon, *POC* particulate organic carbon, *PON* paticulate organic nitrogen, *FDOMm* fluorescence of the dissolved organic matter from marine humic-like substances, *FDOMt* fluorescence of the dissolved organic matter from protein-like substances, *POCp* particulate organic carbon production, *PER* percentage of extracellular release, *Chl-a* chllorophyll-*a*, *BB* bacterial biomass, *BP* bacterial production, *BR* bacterial respiration

were sequentially filtered through 0.8 and 0.2-μm pore size polycarbonate filters and reduced INT (INT formazan) was extracted with propanol and the absorbance at 485 nm was then measured using a spectrophotometer (Beckman model DU640). Respiration of free-living heterotrophic bacteria (i.e., BR) was operationally defined as ETS activity < 0.8 μm [98]. In order to transform INT reduction rates into carbon respiration, an R/ETS ratio of 12.8 [72] and a respiratory quotient (RQ) of 0.89 [117] were used. Detailed methodology for these variables is described elsewhere [109].

## DNA Isolation, PCR, and ARISA Fingerprinting

Samples from 100 and 1% of surface PAR depths at both stations were prefiltered by gravity through a 1.2-μm nominal pore size (Kleenpak Capsule with HDCII filter) to remove eukaryotic cells and particle-associated prokaryotes. Subsequently, 2 L was concentrated for ARISA fingerprinting using low vacuum pressure (< 7 kPa) on a 0.2-μm pore size polycarbonate filters (Nuclepore Whatman, 47-mm filter diameter). Filters were dried, stored in DNAse/RNAse-free centrifuge vials, flash-frozen in liquid nitrogen, and kept at − 80 °C until DNA extraction. DNA was extracted using a phenol-chloroform-isoamyl alcohol extraction protocol as described in [74], modified for polycarbonate filters as follows. After thawing, filters were cut in small fragments using scissors under sterile conditions. Nucleic acid extraction began with the addition of 631.25 μL of lysis buffer (50 mM Tris-HCl, pH = 8.3; 40 mM EDTA, pH = 8; 0.75 M sucrose) with lysozyme (1 mg $mL^{-1}$ final concentration; Sigma-Aldrich), followed by 45-min incubation at 37 °C in slight movement. Then, 18.75 μL of proteinase K (0.2 mg $mL^{-1}$ final concentration; Sigma-Aldrich) and 100 μL of sodium dodecyl sulfate (SDS) (1% *v*/*v* final

concentration) were added, followed by 1-h incubation at 55 °C. Lysate was then washed twice with 1:1 volume of phenol-chloroform-isoamyl alcohol (25:24:1; saturated with 10 mM Tris, pH 8.0, 1 mM EDTA; Sigma-Aldrich) and once with 1:1 volume of chloroform-isoamyl alcohol (24:1; 99% purity for molecular biology; Sigma-Aldrich) and separated by centrifuging at 12,000 rpm 10 min. The aqueous phase was purified and concentrated to a volume of 100 to 200 μL in a microconcentrator (Amicon with Ultracel-100 membrane; Millipore). DNA was transferred from solution to the microconcentrator filter by centrifugation at 3000 rpm and eluted off re-eluted with 2 mL sterilized Milli-Q water (that had been autoclaved and 10 min under UV light). The samples were then re-bound and eluted two more times (for a total of three washing steps). The recovered DNA was quantified in a Nanodrop spectrophotometer and diluted to a working concentration of 10 ng $\mu L^{-1}$ of template DNA and stored at − 20 °C until further analysis. The BCS within every sample was analyzed using ARISA fingerprinting [40]. Extracted microbial community DNA was PCR amplified by using the bacterial-specific internal transcribed spacer forward (ITSF) and reverse (ITSReub) primers set (Cardinale et al., 2004), the former being labeled at the 5′ end with the fluorescein amidite (6-FAM) dye (Thermo Scientific). PCR reactions (40 μL) contained final concentrations of 1× PCR buffer (Genecraft), 2.5 mM $MgCl_2$ (Genecraft), 250 μM of each dNTP (Genecraft), 250 nM of universal primer ITSF (5′-[6-FAM]GTCGTAACAAGGTAGCCGTA-3′) and eubacterial ITSReub (5′-GCCAAGGCATCCACC-3′), 40 ng $\mu L^{-1}$ bovine serum albumin (BSA), 0.063 U $\mu L^{-1}$ of BioThermD™ Taq DNA Polymerase (Genecraft), and 1.125 ng $\mu L^{-1}$ of template DNA. The reaction mixture was held at 94 °C for 2 min, followed by 32 cycles of amplification at 94 °C for 15 s, 55 °C for 30 s, and 72 °C for 3 min, with a final extension of 72 °C for 10 min. Amplified products were sent for capillary electrophoresis migration at Genoscreen (www.genoscreen.fr/). Unfortunately, we were unable to amplify bacterial DNA from samples at the 1% $E_0$ in May and 100% $E_0$ in July and September at A Coruña. Profile peaks were binned and rearranged by operational taxonomic units (OTUs). Only peaks on the range 200 to 1200 bp and relative fluorescence intensity (RFI) values contributing > 0.09% to the total abundance of the sample were considered. We assumed that each peak area associated with each fragment represented the relative abundance of each bacterial OTU within the sample. Bacterial richness was quantified as the number of detectably different OTUs in each standardized sample. Detailed descriptions of the analysis of sample profiles, such as peak calling and quality check, are provided in the Supporting Information. The evenness of the community abundance distribution was estimated using the inverse Simpson's index, which is relatively insensitive to numerically minor constituents [16, 66]. We did not attempt to calculate richness, because ARISA fingerprinting (like most other methods of microbial community analysis) does not detect rare taxa. In this case, we could not detect OTUs representing < 0.1% of the individuals in a sample.

## Statistical Analyses

Differences in physical, chemical, and biological variables, as well as OTU richness and evenness between locations (A Coruña and Vigo), PAR (100 and 1% $E_0$) and hydrographical situation (*Up* and *Dw*) were analyzed on SPSS software applying non-parametric tests [Kruskal–Wallis (K–W) test or Mann–Whitney (M–W) test, with Monte Carlo permutations], because of the non-normal distribution of most of the variables considered. Correlations among microbial community abundances and physical, chemical, and biological variables were calculated by using Spearman's correlation. In case of multiple comparison tests, the *p* value was corrected for the number of comparisons using the Bonferroni method [108].

Multivariate analyses were performed with the software PRIMER6 [29, 30]. Environmental variables were first normalized, and then, Euclidean distances among samples were calculated. The Bray–Curtis similarity of the BCS was calculated from standardized ARISA relative abundances (squared root transformed). The resulting dissimilarity (for environmental variables) and similarity (for BCS) matrices were used to construct a distance-based redundancy analysis (dbRDA) [69]. Permutation multiple analyses of the variance (PERMANOVA) were performed in order to statistically explore whether BCS significantly differ among sample groups [i.e., different locations (L), optical depths (OD), or hydrographic situation (HS)], by comparing Bray–Curtis similarities among samples (all groups together and pairwise comparisons) using an "add-on" package for PRIMER6, PERMANOVA+ [8, 10, 75]. A distance-based test for homogeneity of multivariate dispersions (PERMDISP) was used to verify whether differences found by the PERMANOVA test were due to differences in homoscedasticity (i.e., data dispersion) between pairs of groups, or real differences between data groups in the dbRDA ordination axes [9]. Furthermore, parsimonious models were built to identify the best factors explaining variation in the community structure (distance linear-based model (DistLM) using the stepwise procedure with Akaike's information criterion (AIC) [75]). In order to determine which combination of predictive variables better explain changes in BCS, including seasonal (D-L, Iw, PPT, and UML), environmental (not showing strong correlation with seasonal variables) (T, S, PAR, $PO_4$, $SiO_4$, $NO_3$, $NO_2$, $NH_4$, total dissolved nitrogen (TDN), FDOM*m*, FDOM*t*, DOC, POC, POCp, percentage of extracellular release (PER) and Chl-*a*), and functional (BP, BR and BB), a DistLM was conducted parallel to the dbRDA.

Hierarchical cluster analysis was applied to cluster individual OTUs based on standardized ARISA relative abundances using the group average mode on the PRIMER6 software. Furthermore, correlations between the relative abundance of individual OTUs within the same sampling depth but different location (inter-location) were calculated by using Spearman's correlation coefficient. Those OTUs that were significantly correlated were considered to display spatial synchrony.

To evaluate the relationship between BCS, bacterial carbon cycling (i.e., functionality), environmental factors, and seasonal variability, partial correlations between the corresponding matrices (based on the Bray–Curtis similarity for BCS and on the Euclidean distances for the other groups of matrices) were computed using a Mantel test procedure (partial Mantel tests, two-tailed $p$ values using 999 random permutations) with the PASSaGE v2 software [http://www.passagesoftware.net [100]].

## Results

### Contextual Variables

The upwelling index (Iw), precipitation, and UML depth were all significantly and highly correlated to D-L, and, therefore, considered seasonal variables. The thermohaline variability throughout the sampling period (Supporting Information Fig. S1a, b) was essentially driven by the typical seasonal thermal cycle, winter mixing, and coastal runoff, as well as by upwelling pulses during spring and summer (Fig. 2). Favorable upwelling conditions, as inferred from positive upwelling index (Iw) values, dominated from April to September 2010 at both sampling locations, whereas favorable downwelling conditions (negative Iw values) predominated from January to March 2010 and from October to December 2010 (Fig. 2a). Precipitation (PPT) was seasonal and was highest off Vigo (Fig. 2c). From January to March, freshwater discharges extended onto the shelf adjacent to the Ría de Vigo, leading to temperature inversions associated with the development of a marked halocline (Fig. S1b). In early spring, the increase in solar radiation and water column stratification (Fig. 2b and Supporting Information Fig. S1a, b) promoted phytoplankton growth at both stations, as reflected by increased Chl-$a$ concentration in surface waters (Supporting Information Fig. S1e, f). Strong upwelling pulses during late spring and summer (May–August 2010) favored the advection of cold and nutrient-rich subsurface waters near the surface (Supporting Information Fig. S1c, d). Upwelling intensity was higher off Vigo than off A Coruña during this period (Fig. 2a), where the strongest upwelling pulse occurred in

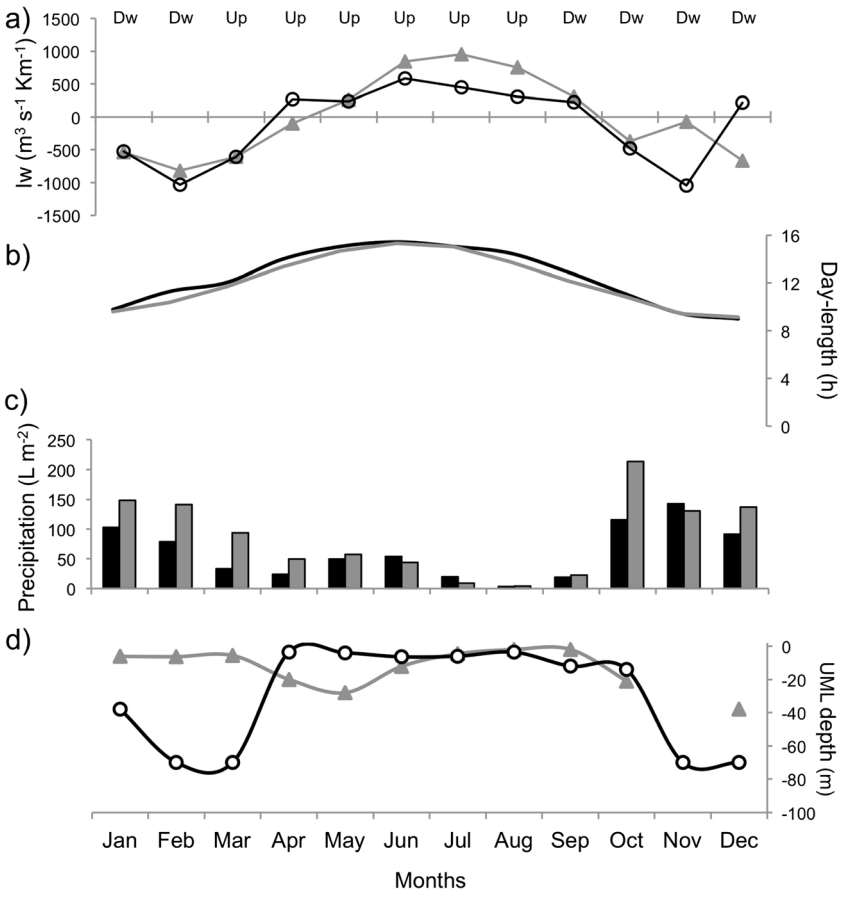


**Fig. 2** Distribution of monthly **a** offshore upwelling index (Iw), **b** day length, **c** precipitation, and **d** UML depth, off A Coruña (black) and Vigo (gray) during the sampling period. Sampling months are classified into upwelling (Up) and downwelling (Dw) periods

August 2010 when water of about 14 °C reached the surface (Supporting Information Fig. S1b). On the other hand, downwelling of shelf surface waters was higher off A Coruña than off Vigo (Fig. 2a), which was reflected by the deeper UML and the homogenization of water column temperature during late autumn and winter (Fig. 2d and Supporting Information Fig. S1a).

Samples were classified into two groups [upwelling/productive period (Up) and downwelling/non-productive period (Dw) periods] according to the hydrographical situation based on both the Iw and the vertical profiles of temperature (T) and Chl-*a* (Fig. 2 and Supporting Information Fig. S1a, b, e, f). The upwelling period includes samples from March to August 2010, and the downwelling period includes samples from January to February 2010 and from September to December 2010 (Fig. 2 and Supporting Information Fig. S1).

Mean water temperature (T) and salinity (S) showed relatively low variation among sample groups, being significantly lower at the 1% of surface photosynthetically active radiation (PAR) depth (hereafter 1% $E_0$ or the base of the euphotic zone) than at the optical depth of 100% of surface PAR (hereafter 100% $E_0$ or surface) during the Up period (Table 1). Mean dissolved organic carbon (DOC) concentration was significantly higher off A Coruña than off Vigo (K–W test, $p = 0.03$, $N = 42$), while particulate organic carbon and nitrogen (POC and PON, respectively) concentrations were significantly higher off Vigo than off A Coruña (K–W test, $p = 0.02$ and 0.006, $N = 46$ and 45, respectively). Off Vigo, DOC, POC, and PON were significantly lower only at the 1% $E_0$ compared with the 100% $E_0$ during the Up period, whereas off A Coruña, POC and PON were significantly lower at the 1% $E_0$ independently of the hydrographic situation (Table 1).

Marine humic-like fluorescence of dissolved organic matter (FDOM*m*) was significantly higher at 100% $E_0$ than at 1% $E_0$ optical depth off Vigo during the downwelling period (M–W test, $p = 0.035$, $N = 10$). Protein-like fluorescence of dissolved organic matter (FDOM*t*) was significantly higher off A Coruña than off Vigo (K–W test, $p = 0.004$, $N = 41$). Chl-*a* concentration was higher at 100% $E_0$ depth and highest during the onset of upwelling period at both locations. Particulate organic carbon production (POCp), bacterial production (BP), and bacterial respiration (BR) followed very similar patterns as Chl-*a* in surface waters at both sites, being higher at 100% $E_0$ at both locations, with the highest rates during the upwelling period. Bacterial biomass (BB) did not differ between hydrographic conditions and was higher off Vigo than off A Coruña (K–W test, $p = 0.007$, $N = 44$) (Table 1).

## Bacterioplankton Diversity

A total of 305 different OTUs were detected (ARISA detection threshold of 0.09%, see "Material and Methods" section) over the sampling period at the two optical depths off A Coruña and Vigo (Table 2), of which only 4 OTUs (~ 1.3%) occurred in all samples (ubiquitous OTUs) whereas 79 (~ 26%) where found only once (unique OTUs, using the 95 percentile of the control as background and considering only the peaks contributing > 0.09% to the total abundance of the sample). In terms of relative abundance, the 4 ubiquitous OTUs accounted, on average, for 27 ± 12.5% (± SD) of the community, whereas the 79 unique OTUs accounted only for 0.59 ± 1% of the community.

In general, A Coruña and Vigo showed a similar number of distinct OTUs, a total of 253 and 245 OTUs, respectively (Table 2). Only 6 and 4 OTUs were present in all the samples and 41 and 38 were unique off A Coruña and Vigo, respectively. OTUs were classified into persistent (found in > 80% of the samples), intermittent (20–80%), and ephemeral (< 20%). Most of the OTUs were ephemeral, although cumulatively represented a small fraction of the community inhabiting the euphotic zone (142 OTUs in A Coruña and 128 OTUs in Vigo, accounting for < 10% of the community). Many OTUs were intermittent (90 and 93, accounting for about 35% of the community at both locations). Fewer than 10% of OTUs were persistent at each location along the year (21 and 24 OTUs, respectively, accounting for > 60% of the community) (Table 2).

The cumulative number of ephemeral OTUs was higher off A Coruña than off Vigo (142 and 128, respectively). At both locations, the cumulative number of ephemeral OTUs in surface waters was higher than at the base of the euphotic zone (A Coruña: 100% $E_0 = 107$, 1% $E_0 = 90$; Vigo: 100% $E_0 = 109$, 1% $E_0 = 81$). Also, at the base of the euphotic zone, the cumulative number of ephemeral OTUs was higher during downwelling conditions also at both locations (A Coruña 1% $E_0$: Up = 48, Dw = 77; Vigo 1% $E_0$: Up = 37, Dw = 60; Table 2). Persistent OTUs, on the other hand, were more abundant at the 1% $E_0$ depth than in surface waters, especially off Vigo (A Coruña: 100% $E_0 = 22$, 1% $E_0 = 33$; Vigo: 100% $E_0 = 20$, 1% $E_0 = 46$). In both cases, persistent OTUs showed a higher number during the downwelling period than the upwelling period, though their contribution to the community was similar during both hydrological periods (Table 2).

Considering the whole annual cycle, 63% of the detected OTUs were present at both locations. The percentage of shared OTUs between locations within the same optical depth was similarly high (approximately 62%). Within each location, the percentage of shared OTUs between sampling depths was also high (58% off A Coruña and 61% off Vigo).

The temporal variability in bacterial diversity was, both in terms of bacterial richness (number of distinct OTUs) and evenness (inverse Simpson's index), similar off A Coruña and Vigo, yet some differences between sampling depths and periods were found (Fig. 3, Table 3). Samples from 1% $E_0$ depth were, in terms of both richness and evenness, slightly more diverse than those from 100% $E_0$ depth at both locations

**Table 2** Number of distinct total OTUs (Total OTUs) at the two sampling sites (A Coruña and Vigo) for the two optical depths [100 and 1% of surface photosynthetically active radiation ($E_0$)] during upwelling (Up) and downwelling (Dw) periods. For each of these groups, the number of persistent, intermittent, and ephemeral OTUs (by the corresponding group) is given together with the mean relative community abundance (± SD) they collectively represent

| Groups of samples | | | Total OTUs | | | Persistent | | | Intermittent | | | Ephemeral | | | Number | |
|---|---|---|---|---|---|---|---|---|---|---|---|---|---|---|---|---|
| Location | PAR | Hydrog. situation | | | | OTUs (% of community) | | | OTUs (% of community) | | | OTUs (% of community) | | | (samples) | |
| A Coruña | 100% E0 | Up | 253 | 204 | 142 | 21 (60 ± 12) | 22 (63 ± 9) | 26 (74 ± 8) | 90 (34 ± 10) | 75 (29 ± 9) | 50 (17 ± 1) | 142 (6 ± 5) | 107 (7 ± 6) | 66 (9 ± 8) | 21 | 11 | 5 |
| | | Dw | | | 164 | | | 32 (72 ± 2) | | | 69 (26 ± 2) | | | 63 (4 ± 0) | | | 6 |
| | 1% *E0* | Up | | 196 | 138 | | 33 (69 ± 12) | 37 (80 ± 11) | | 73 (25 ± 11) | 53 (16 ± 9) | | 90 (6 ± 3) | 48 (4 ± 2) | | 10 | 5 |
| | | Dw | | | 169 | | | 47 (72 ± 8) | | | 45 (20 ± 6) | | | 77 (8 ± 4) | | | 5 |
| Vigo | 100% *E0* | Up | 245 | 199 | 131 | 24 (60 ± 12) | 20 (64 ± 14) | 20 (72 ± 13) | 93 (35 ± 9) | 70 (29 ± 10) | 53 (24 ± 10) | 128 (4 ± 4) | 109 (7 ± 6) | 58 (5 ± 4) | 22 | 11 | 6 |
| | | Dw | | | 149 | | | 31 (71 ± 8) | | | 57 (23 ± 8) | | | 61 (6 ± 3) | | | 5 |
| | 1% *E0* | Up | | 195 | 139 | | 46 (78 ± 7) | 47 (80 ± 10) | | 68 (18 ± 5) | 55 (16 ± 7) | | 81 (5 ± 4) | 37 (3 ± 4) | | 11 | 6 |
| | | Dw | | | 164 | | | 50 (81 ± 4) | | | 54 (14 ± 3) | | | 60 (4 ± 4) | | | 5 |
| All samples | | | 305 | | | 2223 (60 ± 12) | | | 89 (35 ± 9) | | | 193 (5 ± 5) | | | 43 | | |

(Fig. 3). Such differences were significant off Vigo (M–W test, $p = 0.039$ and 0.003 for richness and evenness, respectively, $N = 22$) (Table 3). Similarly, diversity was significantly higher during downwelling than during upwelling periods (richness: M–W test, $p = 0.013$, $N = 43$; evenness: M–W test, $p = 0.009$, $N = 43$) (Fig. 3, Table 3).

OTU richness declined from January to April at both locations and depths. In April, richness off A Coruña were 0.2 and 0.7-fold lower than annual mean values at 100% $E_0$ and 1% $E_0$ depths, respectively (Fig. 3a). Off Vigo, April samples were 0.28 and 0.32-fold lower than annual mean values at 100% $E_0$ and 1% $E_0$, respectively (Fig. 3b). Then, richness increased in the 1% $E_0$ depth at both locations, as the Iw intensity became stronger, reaching a maximum in June, followed by a slight decrease during the rest of the Up period. After that, richness increased, reaching values as high as in June between October and December. A moderate increase was also observed in surface samples.

Bacterial evenness in surface samples was more stable off A Coruña compared with Vigo, where evenness was highly variable throughout the year (Fig. 3c, d). At the 1% $E_0$ optical depth off A Coruña, evenness increased from February to March, but sharply decreased from March to April, reaching a minimum value. After that, bacterial evenness recovered throughout the summer, increasing again during the Dw period. A similar pattern, although less marked, was also observed at the surface.

Bacterial evenness off Vigo followed similar patterns at the surface than at the 1% $E_0$ optical depth. A sharp decline occurred from January to February and from February to March at the 100 and 1% $E_0$ optical depths, respectively. After that, bacterial evenness moderately recovered, until a sharp increase occurred from May to June only at the 1% $E_0$. Bacterial evenness at the 100% $E_0$ had a moderate decrease from June to September, which was more pronounced at the 1% $E_0$ optical depth.

## Spatial and Temporal Patterns in Bacterial Community Structure

A distance-based redundancy analysis (dbRDA) based on Bray–Curtis similarities between samples showed that the BCS was strongly influenced by the hydrographical situation and by the optical depth, but not by the sampling location (Fig. 4, Supporting Information Table S1). A high similarity of BCS was found among samples from the downwelling period independently of location or depth, whereas the BCS of samples from the upwelling period grouped according to the optical depth (independently of the location) (Fig. 4, Supporting Information Table S2).

When comparing the BCS similarity between groups of samples from the same hydrographical situation and optical depth from A Coruña with those from Vigo, it becomes more

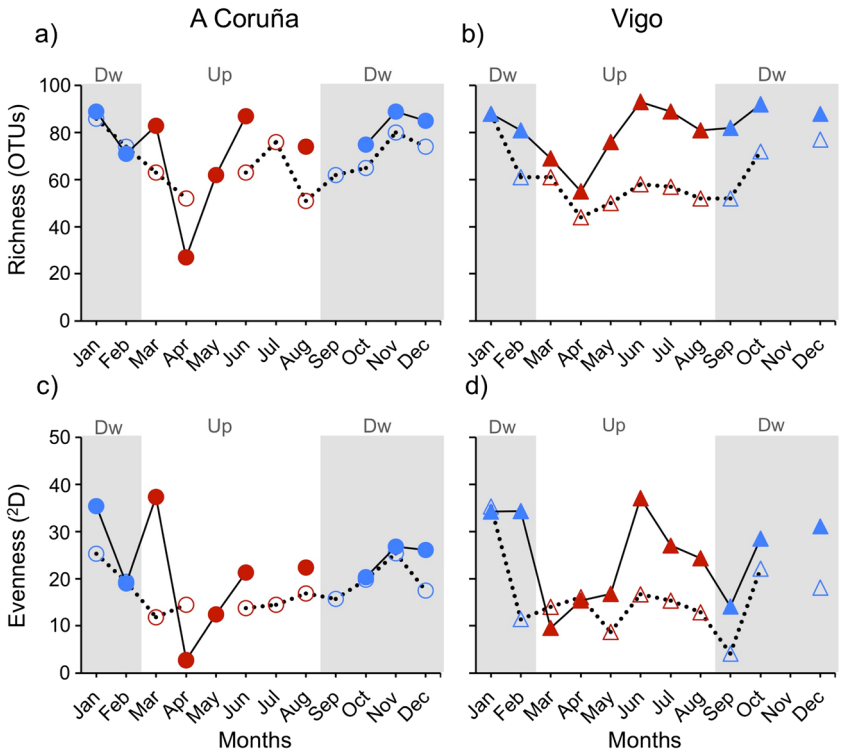


**Fig. 3** Temporal variation in richness (number of distinct OTUs) off **a** A Coruña and **b** Vigo and evenness [inverse Simpson's index ($^2D$)] off **c** A Coruña and **d** Vigo (circles and triangles, respectively). Open and filled symbols represent 100% $E_0$ and 1% $E_0$ depth samples, respectively. Blue and red symbols represent downwelling and upwelling samples, respectively. Shaded gray areas indicate months from the downwelling period

evident that location has little effect on BCS, as there were no significant differences between groups (Fig. 4, Supporting Information Table S2).

Individually, most of the contextual variables significantly explained part of the variability on the BCS matrix, and up to 12 variables explained more than 10% of this variability (Table S3). The best DistLM solution included nine significant variables that predicted the bacterial assemblages (Table 4). These variables explained up to 53.6% of the fitted model variation, with seasonal variables (day length and precipitation) explaining up to 19.6% of this variability (Table 4, Fig. 4).

The dbRDA plot showed that changes in day length and precipitation mostly explained differences in bacterial communities under upwelling and downwelling conditions. Temperature and phosphate, and to a lower extent Chl-*a*, PER, and FDOM*m*, were most strongly associated with differences in bacterial communities at different optical depths (Fig. 4).

To evaluate how physical processes connect bacterial communities inhabiting the surface and deeper layers in the euphotic zone, we explored the relationship between the Bray–Curtis similarity of communities inhabiting the 100 and 1% $E_0$ depths (inter-depth similarity) and the UML depth at each

**Table 3** Mean richness and evenness (±SD) at the two sampling sites (A Coruña and Vigo) for the two optical depths [100 and 1% of surface photosynthetically active radiation ($E_0$)] during the two hydrographical situations (HS): upwelling (Up) and downwelling (Dw). Groups of samples with no significant differences (M–W test, Monte Carlo permutations) are indicated with the same super index ($a > b > c$)

| Place | PAR | HS | Richness | | | Evenness | | | Number | | |
|---|---|---|---|---|---|---|---|---|---|---|---|
| | | | (OTUs) | | | ($^2D$) | | | (samples) | | |
| A Coruña | 100% $E_0$ | Up | 71 ± 15 | 68 ± 11bc | 61 ± 10cd | 20 ± 8 | 18 ± 4ab | 14 ± 2bc | 21 | 11 | 5 |
| | | Dw | | | 73 ± 9bc | | | 20 ± 4a | | | 6 |
| | 1% $E_0$ | Up | | 74 ± 19ab | 67 ± 24abcd | | 22 ± 10ab | 19 ± 13a | | 10 | 5 |
| | | Dw | | | 82 ± 8ab | | | 25 ± 7a | | | 5 |
| Vigo | 100% $E_0$ | Up | 71 ± 16 | 61 ± 13c | 54 ± 6d | 20 ± 10 | 16 ± 8b | 14 ± 3c | 22 | 11 | 6 |
| | | Dw | | | 70 ± 14abcd | | | 18 ± 12a | | | 5 |
| | 1% $E_0$ | Up | | 81 ± 11a | 77 ± 14abc | | 25 ± 9a | 22 ± 10ab | | 11 | 6 |
| | | Dw | | | 86 ± 5a | | | 28 ± 8a | | | 5 |
| All samples | | | 71 ± 15 | | | 20 ± 9 | | | 43 | | |

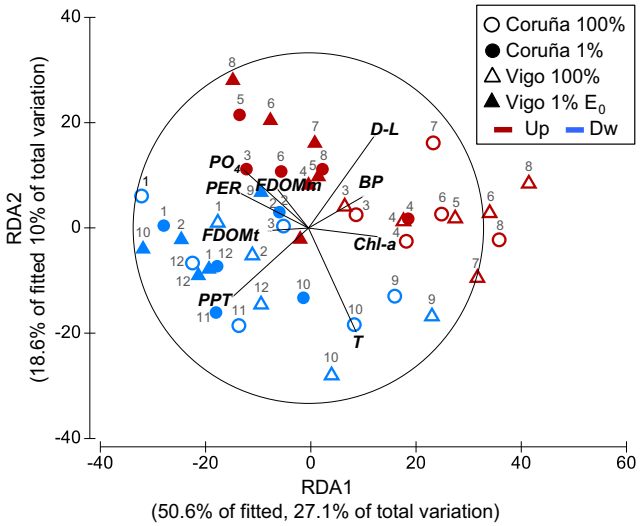


**Fig. 4** Distance-based redundancy analysis (dbRDA) ordination of bacterial community structure based on Bray–Curtis similarity. Samples from A Coruña 100% $E_0$ (open circles) and 1% $E_0$ (filled circles) and Vigo at 100% $E_0$ (open triangles) and 1% $E_0$ (filled triangles). Blue symbols represent samples under downwelling situation, and red symbols represent samples under upwelling situation. Numbers correspond to the 12 months of the year. Only environmental variables that explained variability in microbial community structure selected in the DistLM model (stepwise selection procedure with AIC selection criterion) were fitted to the ordination. BP bacterial production, Chl-*a* chllorophyll-*a*, D-L day length, FDOM*m* fluorescence of the dissolved organic matter from humic-like substances, FDOM*t* fluorescence of the dissolved organic matter from protein-like substances, PER percentage of extracellular release, $PO_4$ phosphate, PPT precipitation, T temperature

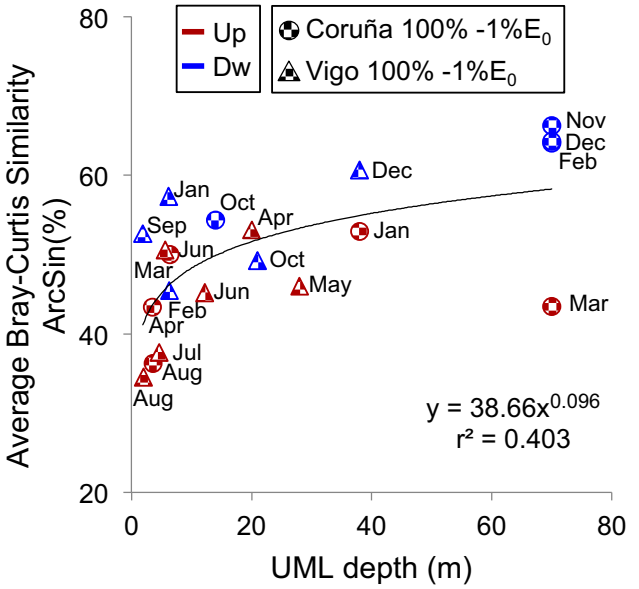


**Fig. 5** Relationship between the similarities (Bray–Curtis similarity) of the bacterial communities inhabiting at 100 and 1% $E_0$ optical depths (100–1% $E_0$) with the upper mixed layer (UML) depth; note that percentage of Bray–Curtis similarities is on an arcsine scale. Circles represent data from A Coruña and triangles from Vigo. Colors correspond to the hydrographical situation (upwelling months in red and downwelling months in blue)

location and sampling time (Fig. 5). A positive relationship ($r^2 = 0.4$, $p < 0.001$) was found between the inter-depth similarity and the UML depth. Bacterial community off A Coruña in March showed a much lower inter-depth similarity compared to other sampling months with similar UML depths.

To further explore the temporal variability of the BCS, we plotted the Bray–Curtis pairwise similarity of samples against time lag (see, for example, [28, 60, 34] at each depth and sampling location (Fig. 6). Bray–Curtis similarity (± SD) off A Coruña was on average 49.8 ± 10.0 and 50.8 ± 9.4% at 100% $E_0$ and 1% $E_0$ depths, respectively. Bacterial communities off Vigo were on average 45.6 ± 12.1 and 58.1 ± 8.5% similar at 100% $E_0$ and 1% $E_0$ depths, respectively. Overall, the highest pairwise Bray–Curtis similarity occurred between communities 1 month apart (a similarity of 70% off A Coruña at both depths and 79% in Vigo at 1% $E_0$), except for Vigo at 100% $E_0$ depth, where maximum similarity occurred between communities 11 months apart (Fig. 6). At both sampling locations and depths, there was a general decrease in the similarity of BCS as more time elapsed, until 5 to 7 months had elapsed. Then, the similarity between communities increased until the end of the time series (11 months after the start), when BCS similarity reached values as similar to those as between samples collected only 1 month apart (Fig. 6).

**Table 4** Sequential test of the predictive variables that better explain the variability of the BCS resemblance matrix by a distance linear model (DistLM) test

| Variable | AIC | SS (trace) | Pseudo-*F* | *p* | Explained variability (%) | Cumulative (%) |
|---|---|---|---|---|---|---|
| D-L | 306.72 | 9728.4 | 8.1265 | 0.001 | 16.5 | 16.5 |
| T | 302.53 | 6583.0 | 6.1959 | 0.001 | 11.2 | 27.7 |
| Chl-*a* | 300.53 | 3776.0 | 3.803 | 0.001 | 6.4 | 34.2 |
| BP | 300.47 | 1807.3 | 1.8604 | 0.067 | 3.1 | 37.2 |
| $PO_4$ | 298.60 | 3182.6 | 3.4909 | 0.002 | 5.4 | 42.6 |
| PPT | 298.22 | 1811.9 | 2.0434 | 0.010 | 3.1 | 45.7 |
| FDOM*t* | 298.15 | 1504.9 | 1.7317 | 0.044 | 2.6 | 48.3 |
| PER | 297.94 | 1522.2 | 1.7912 | 0.031 | 2.6 | 50.9 |
| FDOM*m* | 297.46 | 1615.5 | 1.9543 | 0.026 | 2.7 | 53.6 |

Clustering of OTUs according to their relative abundance profiles showed contrasting temporal variability patterns (Fig. 7). Some OTUs were persistently abundant at both sampling depths and locations (cluster A), whereas others were only abundant either in surface waters (cluster B, Fig. 7) or at the base of the euphotic zone (cluster F, Fig. 7). Some OTUs showed clear seasonal patterns at both optical depths (e.g., cluster B or C, Fig. 7 and Supporting Information Tables S4 and S5), whereas others showed more evident seasonal patterns only in surface waters (e.g., cluster A or H, Fig. 7 and Supporting Information Tables S4 and S5).

Most seasonal OTUs correlated with D-L and precipitation, followed by Iw and the UML depth (Supporting Information Table S4). The number of seasonal OTUs at the base of the euphotic zone off A Coruña was lower than in the surface (Supporting Information Table S4). Conversely, a similar percentage of seasonal OTUs was found at both sampling depths off Vigo (Supporting Information Table S4). Moreover, 52% of the persistent and intermittent OTUs showed significantly correlated temporal patterns inter-locations (between sampling locations at the same depth, Supporting Information Table S5), which suggest spatial synchrony (Fig. 7). In addition, most of the OTUs showing spatial synchrony were also seasonal (Supporting Information Table S5). Some ephemeral OTUs appeared to be also synchronized, producing

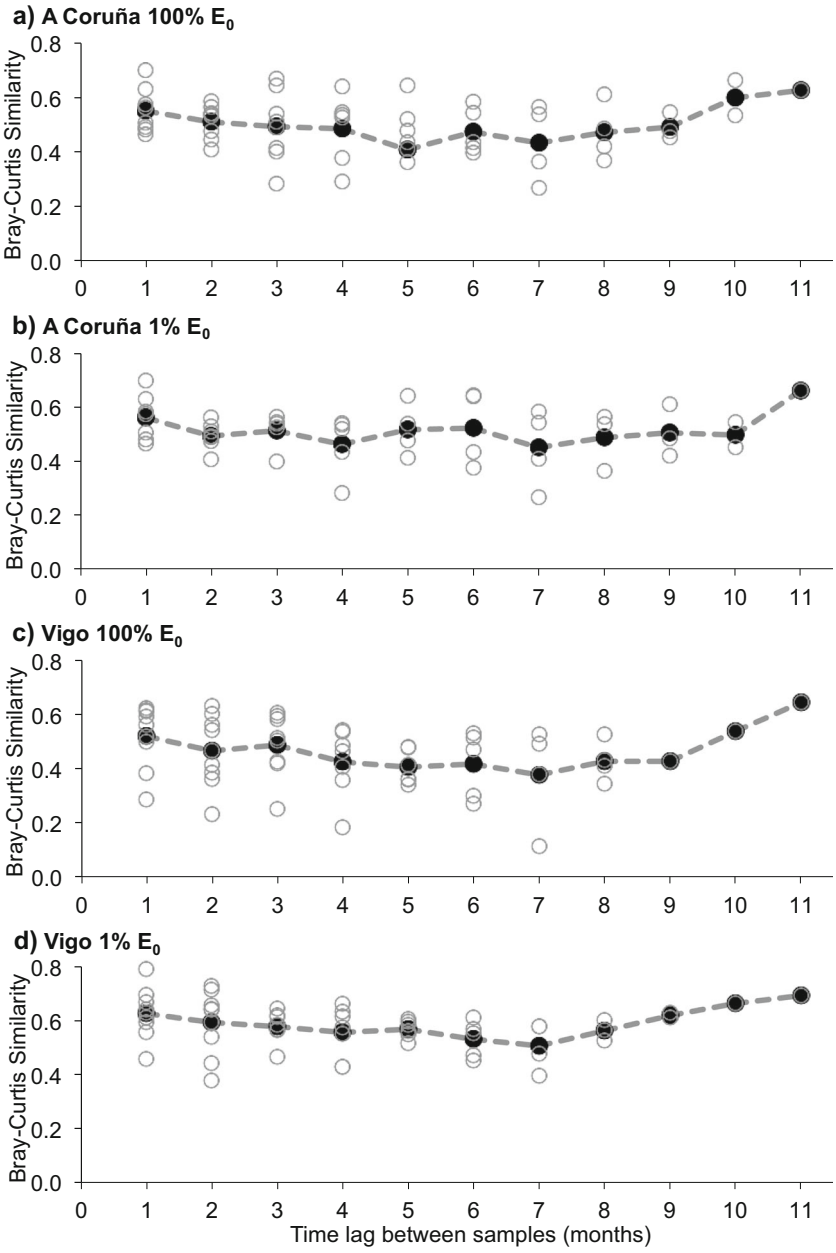


**Fig. 6** Temporal patterns in pairwise Bray–Curtis bacterial community similarity between samples collected *N* months apart. Average pairwise community similarity (*Y*-axis) was calculated for samples **a** off A Coruña at 100% $E_0$ depth, **b** off A Coruña at 1% $E_0$ depth, **c** off Vigo at 100% $E_0$ depth, and **d** off Vigo at 1% $E_0$ depth. Time lag (*X*-axis) indicates the number of months between the pairwise comparisons. Gray circles represent individual pairwise comparisons. Black circles and dash red line represent the mean similarity of all pairs of samples taken a given number of months apart (e.g., the first circle is the mean Bray–Curtis similarity of all pairs of samples taken 1 month apart; the second circle is the mean similarity of all pairs of samples taken 2 months apart, and so on)

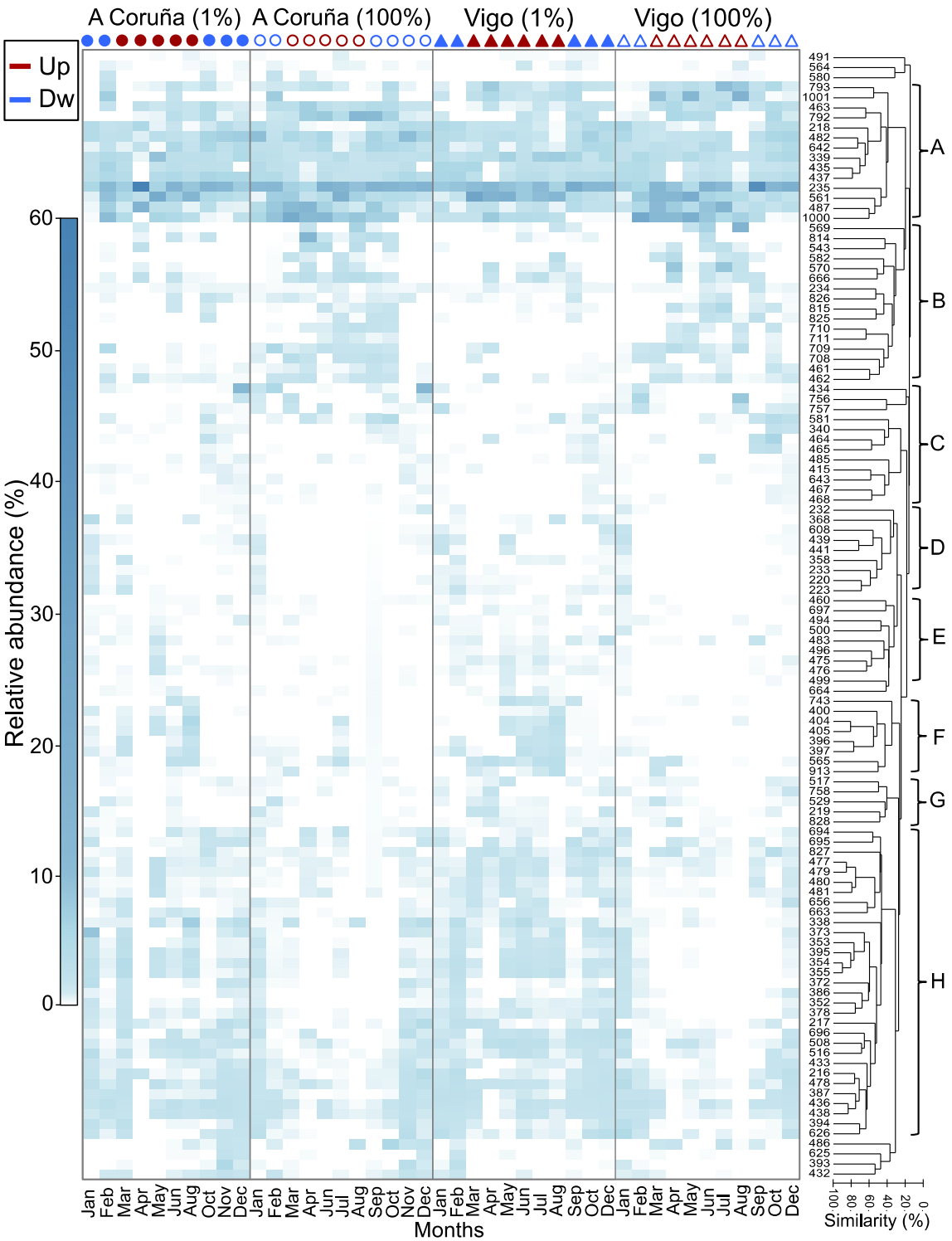


**Fig. 7** Heat map of relative abundances of persistent and intermittent OTUs at each sampling point and time. Each column represents a sequential sample along an annual cycle. Filled symbols represent samples from the 1% $E_0$ optical depth, and open symbols represent samples from 100% $E_0$. Circles represent samples from A Coruña, and triangles represent samples from Vigo. Blue symbols represent samples under downwelling conditions, and red symbols represent samples under upwelling conditions. Each row represents a different OTU. The dendogram represent clustering of OTUs based on their relative abundance profiles. White to blue colors represent relative abundance of OTUs

episodic "blooms" at the same time and depth at both sampling sites (Supporting Information Fig. S2).

### Relationship Between Bacterial Community Structure, Functionality, Seasonality, and Environmental Selection

The relationship between BCS, carbon fluxes mediated by bacterial communities (functionality), and the seasonal and environmental factors was assessed examining correlation of the four resemblance matrices. Resemblance matrices were constructed including samples from the same depth independently of the location, as significant differences in BCS were observed between the two sampling depths ($p < 0.001$) but not between sampling locations ($p = 0.097$; Supporting information Table S1). A significant partial correlation was found between BCS and functionality (carbon fluxes mediated by bacterial communities) ($r = -0.391$), environment ($r = -0.381$), and seasonality ($r = -0.542$) in surface waters. By contrast, the only significant partial correlation between functionality and environmental variables was found at the base of the euphotic zone ($r = 0.429$). At this depth, seasonality did not have a significant effect on the bacterial community after factoring out the effect of the environment (Fig. 8).

## Discussion

### Methodological Considerations

ARISA primers target the intergenic transcribed spacer (ITS) region, which separates the 16S and 23S rRNA genes of many bacteria. This region is widely recognized for its sequence and length hypervariability [19, 20, 59] and encompasses more neutral variation than the 16S rRNA gene, which makes ARISA a well-suited technique to analyze marine microbial community structure data. Recent studies have demonstrated the capacity of ARISA to detect the same community patterns observed with next-generation 16S rRNA gene sequencing techniques [28, 82, 34, 33, 97], and even better at differentiating certain ecotypes of cyanobacteria [99, 19] or SAR11 [22], which are difficult to resolve by 16S rRNA sequence alone [28, 34].

ARISA fingerprinting technique only detects OTUs that make up at least 0.09% of the microbial community and thus do not detect what Sogin et al. [107] would define as microbes from the "rare biosphere." Despite this, the communities that we observed each month showed the typical skewed abundance distribution (few OTUs accounting for most of the abundance and a large tail of less abundant OTUs [89]. It is nevertheless important to consider that even though our

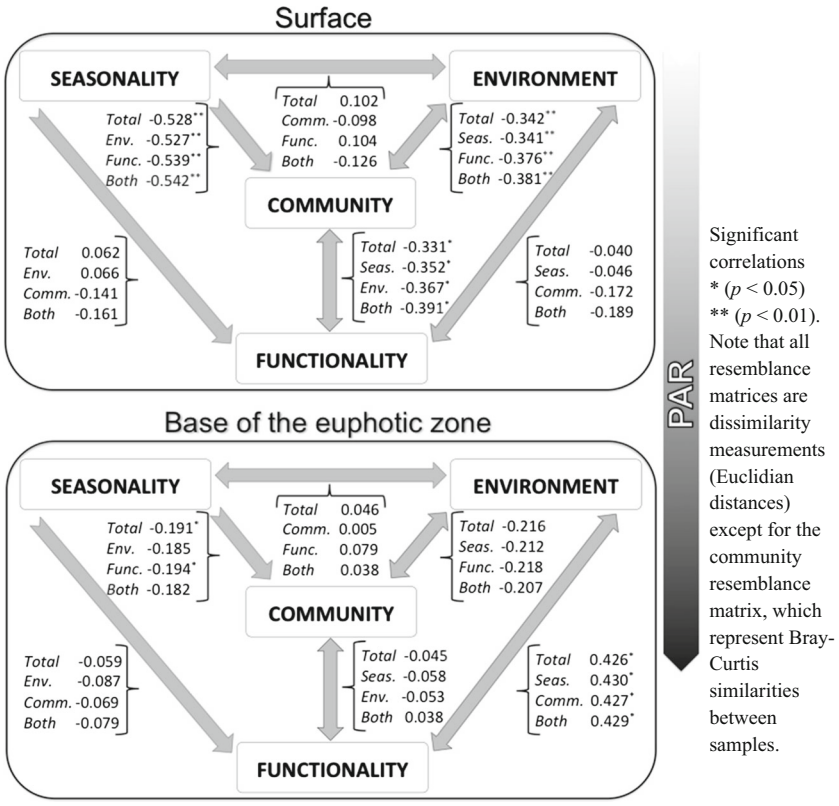


**Fig. 8** Diagram showing the relationship between seasonal, environmental, and functional-related variables with bacterial communities. *Rho* values for the six pairs of comparisons between the four resemblance matrices before (*Total*) and after factoring out the effects of the other matrices: seasonality (*Seas.*), environment (*Env.*), functionality (*Func.*), bacterial community (*Comm.*), and the two factors affecting the two matrix under evaluation (*Both*)

Significant correlations * ($p < 0.05$) ** ($p < 0.01$). Note that all resemblance matrices are dissimilarity measurements (Euclidian distances) except for the community resemblance matrix, which represent Bray-Curtis similarities between samples.

relative abundance estimates may have biases toward some taxa, any bias is consistent from sample to sample, supporting the conclusions drawn from the seasonal dynamics. In addition, the statistical analyses used to find patterns in this study are generally insensitive to such biases.

Even though our dataset only covers a single annual cycle, and a few samples were unfortunately lost because of stormy weather and methodological issues, the strong and significant correlations among individual OTUs relative abundances and seasonal variables indicate a good coverage for this sampling period.

## Bacterioplankton Diversity

We detected more than 300 distinct OTUs including both locations and sampling depths along the annual cycle. This recovery is only slightly lower than that observed in longer time series where the same technique was applied ([19, 28, 33], which is likely related to the greater number of samples in these previous studies. The average richness per sample, however, was very similar to that previously reported [19, 28, 82, 33].

The proportion and abundance of persistent, intermittent, and ephemeral OTUs was similar at both locations, and comparable to previous studies in other oceanic regions, such as the Western English Channel [54], the Hawaii Ocean Time Series (HOT) station [37], and San Pedro Ocean Time series (SPOT) station [28]. The lower number of ephemeral OTUs at the base of the euphotic zone compared with surface waters suggests a higher environmental stability (Table 2). On the other hand, the large number of ephemeral OTUs observed at the 1% $E_0$ optical depth during downwelling conditions could be related with the eventual transport of offshore surface OTUs down to the base of the euphotic depth.

Similar levels and temporal fluctuations of bacterial diversity were observed at both locations (Fig. 3). Surface upwelling waters were more productive [109] but less diverse than waters at the base of the euphotic zone, both in terms of richness and evenness (Fig. 3, Table 3). Previous studies in temperate marine ecosystems [3, 28, 37, 38, 45, 50, 54] and bacterial distribution models [65] reported and predicted, respectively, an increase in diversity during winter. The vertical reshuffling of bacterial taxa due to winter mixing [33, 50] and strong competition during stratified oligotrophic conditions may drive the observed temporal patterns. The intermediate conditions between winter mixing and summer stratification (i.e., spring and autumn seasons) are very productive periods (bloom periods) when certain species (r-strategists) can quickly take up nutrients and bloom. This may explain the sharp decrease in richness and evenness during early spring (February to April), and, although less marked, during late summer early autumn (August–September) at both locations and depths (Fig. 3).

## Spatial and Temporal Patterns of Bacterial Communities

BCS was remarkably similar at the two sampling locations (Fig. 4, Supporting Information Tables S1, S2), with a considerable fraction (> 50%) of persistent and intermittent OTUs (Fig. 7) showing temporal coherence (i.e., spatial synchrony). In the absence of dispersal, spatial synchrony among populations is often attributed to extrinsic climatic drivers, the so-called Moran effect [78, 101] or to trophic interactions with populations that exhibit spatial synchrony [70]. The fact that most of the OTUs showing spatial synchrony were also seasonal (Supporting information Table S5), and the relatively low connectivity between sampling locations at relevant temporal scales, suggests that synchrony is mainly forced by external factors. To the best of our knowledge, similar patterns of spatial synchrony between sampling locations have not been previously described in marine microbial ecosystems and reinforces the idea of a BCS mainly driven by regional seasonal factors rather than by biotic interactions [55]. An alternative explanation for the high horizontal spatial similarity of bacterial communities would be the effect of the Iberian Poleward Current (IPC) on dispersal. This agrees with the higher similarity observed between locations during the winter period (Fig. 6). During the winter, the southerly winds promote the surface northward flow of warm and saline water on the slope, turning right off Cape Finisterre to enter the Rías Altas [6, 25, 26], eventually promoting the connectivity of bacterial communities between the Rías Baixas and the Rías Altas.

Some ephemeral OTUs showed episodic blooms, probably in response to favorable environmental changes. However, since these OTUs were only detectable by our ARISA method during one or two time points, we were not able to identify any robust statistical associations between these blooms and environmental parameters. Intriguingly, some ephemeral taxa also bloomed in synchrony at both locations and/or depths (Supporting Information Fig. S2), which suggests that they may be responding to processes occurring at regional or larger scales, such as annual phytoplankton and nutrient cycles, precipitation events, or upwelling downwelling episodes. Several recent studies have found a wide diversity of rare taxa that have a “boom and bust” abundance patterns; these are often called conditionally rare taxa (CRT) or pulse populations [3, 71, 105]. Furthermore, many of these CRT have been previously shown to exhibit synchronous dynamics [3].

A clear differentiation of BCS was found between the two sampling depths, in agreement with previous studies where microbial abundance and species distribution have been found to vary vertically (e.g., [23, 28, 48, 52, 55, 91–92, 33, 57). The primary cause of this variability is the availability of light and nutrients. Planktonic communities inhabiting the euphotic zone are mainly driven by the input of solar energy, that confines primary production

to surface waters and geographical regions and seasons where light is abundant. Nevertheless, the differences between depths were not significant during the downwelling period (Supporting Information Table S2), suggesting that both depths were homogenized by vertical mixing, particularly during winter months. The significant correlation between the Bray–Curtis similarity inter-depths (i.e., similarity of communities inhabiting the 100 and 1% $E_0$ depths) and the UML depth (Fig. 7) reinforces the role of physical forces in this upwelling system. In summer, as the euphotic zone becomes stratified and environmental conditions change at the surface and at the base of the euphotic zone, bacterial communities diverge, as previously reported at SPOT and BATS [23, 28, 80, 113, 33], but not at Station ALOHA, where the oligotrophic water column is permanently stratified and the mixing is much less seasonally dynamic [36]. The relatively low inter-depth similarity observed in March in A Coruña regardless of a wide UML could be explained by the influence of the phytoplankton growth occurring in upper water column associated with the seasonal increase in light intensity and D-L (Fig. 2 and Supporting Information Fig. S1e).

## Seasonality of Bacterial Communities

Seasonal dynamics in plankton communities are of particular relevance because seasonal patterns can tell us about potential effects of future changes in global climate [56]. Previous work in our study area has shown a marked seasonality for several physicochemical variables [6, 35, 85, 87] as well as planktonic communities inhabiting the euphotic zone [6, 17, 18, 24].

Temporal patterns shown by both the overall community and individual OTUs (Figs. 6 and 7), and the large fraction of persistent (74%) and intermittent OTUs (71%) which monthly relative abundances significantly correlated with seasonal variables (Supporting Information Tables S4, S5), strongly suggest seasonal dynamics. Seasonal variability seems to be largely forced by extrinsic regional factors, such as day length and precipitation (Fig. 4, Table 4) and the winter mixing [103]. Seasonality has been observed in other temperate regions [3, 23, 28, 32, 34, 49, 80, 113, 116] and attributed to seasonal changes in temperature, nutrients, and day length or to interactions with other microbial or larger organisms populations similarly affected by seasonal environmental factors. Given that the effects of most seasonal environmental factors are attenuated with depth, one would expect to observe a decrease in seasonal patterns of bacterial communities with depth. Accordingly, the effect of seasonality in BCS was less apparent at the base of the euphotic depth (Fig. 8, Supporting Information Tables S4 and S5), in accordance with previous findings at HOT (Hawaii Ocean Time Series) and BATS (Bermuda Atlantic Time Series Study) reviewed in [56] and SPOT (San Pedro Oceanographic Time Series) [28, 33].

## Linkages Between Bacterial Community Structure, Seasonal, and Environmental Factors and Functionality

DOC degradation by heterotrophic bacteria has important ecosystem implications as it determines the fate of carbon in the ocean [15]. This process is commonly dependent on the bioavailability of DOC and the concentration of inorganic nutrients and/or other abiotic factors (e.g., temperature). Over the last decade, several studies have investigated the link between BCS and function but have generated contrasting results. Some studies report a significant correlation between BCS and function [4, 110]. Others suggest a large degree of functional redundancy of bacterial communities, as changes in structure are not related with changes in bacterial function (e.g., [12, 67, 68, 102]). However, there were methodological differences between these studies: Lear et al. [68] and Ruiz-González et al. [102] investigated the carbon assimilation potential of microbial communities using 31 different carbon sources as a proxy for bacterial function, while the others used direct measurements of carbon utilization (i.e., bacterial production and/or respiration).

In order to relate BCS with function, we here estimated both bacterial production and respiration. We additionally separated the effect of clearly seasonal variables, such as day length, precipitation, the upper mixed layer, and the upwelling index, from that of other environmental variables so as to distinguish the effect of climatic factors (i.e., regional factors) from that of intrinsic factors (i.e., local factors) on the structure of the bacterial community, as well as on its functionality (independently of each other). Partial Mantel tests revealed that surface bacterial communities are strongly affected by seasonality and by local environmental factors, although the correlation was stronger with regional seasonal factors (Fig. 8), as previously observed in other temperate coastal systems (e.g., [55]). Interestingly, bacterial functionality was only significantly correlated with bacterial community structure, in contrast with other studies where both the environment and the composition affected bacterial function [110]. While changes in surface bacterial communities are largely predictable, since much of the variation is seasonal, bacterial communities at the base of the euphotic zone do not seem to be as predictable. Although we found a certain degree of seasonality in the BCS at the base of the euphotic zone at both sampling locations (Fig. 7, Supporting information Tables S4 and S5), the lack of correlation when pooling data from both locations and factoring out the effect of non-seasonal environmental variables (Fig. 8) suggests that seasonality may be less relevant than in surface waters. Functionality at the base of the euphotic zone was only significantly related with local environmental conditions, likely reflecting more diverse and stable communities well adapted to episodic substrate availability (e.g., DOC flux associated to winter mixing).

In summary, as has been previously observed in other temperate regions, bacterial diversity and community structure show clear vertical and seasonal patterns in this coastal upwelling ecosystem. Our study additionally suggests that horizontal homogeneity and synchrony of bacterial communities is seemingly linked to regional factors, such as upwelling–downwelling dynamics, although it is not possible to exclude dispersal being an important factor. Seasonal mixing, largely associated to downwelling conditions and winter mixing, disrupts vertical heterogeneity and increases bacterial diversity and community similarity between depths and locations. Moreover, bacterial-mediated carbon fluxes in this productive region appear to be best predicted by bacterial community structure in surface waters, whereas local environmental factors are better predictors of bacterial function at the base of the euphotic zone. The three dimensions (horizontal space, depth, and time) considered here add significant value at understanding and forecasting microbial diversity patterns (e.g., seasonality, co-occurrence, spatial synchrony), which might be related to key functional roles in an ever changing world.

**Acknowledgements** We thank all the people involved in the projects DIFUNCAR and RADIALES who helped sampling and the analytical work. We thank the crew of the R/V Lura and R/V J. M. Navaz for their help during the work at sea. POC analyses were made at the analytical facilities (SAI) of the Universidade da Coruña (Spain) and FDOM analyses were performed by Dr. P. Álvarez-Salgado at the IIM of Vigo. G. Casas, A.F. Lamas M. P. Lorenzo, and F. Rozada assisted with water sampling and filtration, F. Eiroa with flow cytometry analysis, MJ Pazo with fluorescence and DOM analyses, and V Vieitez with nutrient analyses. This research was supported in part by the MEC project DIFUNCAR (CTM2008-03790/MAR) and by IEO projects RADIALES. V.H-M. was funded by a FPI MICINN fellowship (BES-2009-028186), and E.T. was founded by a Ramón y Cajal-MEC contract.

## Compliance with Ethical Standards

**Conflict of Interest** The authors declare that they have no conflict of interest.

## References

1. Acinas SG, Rodríguez-Valera F, Pedrós-Alió C (1997) Spatial and temporal variation in marine bacterioplankton diversity as shown by RFLP fingerprinting of PCR amplified 16S rDNA. FEMS Microbiol Ecol 24:27–40
2. Alonso-Gutierrez J, Lekunberri I, Teira E, Gasol JM, Figueras A, Novoa B (2009) Bacterioplankton composition of the coastal upwelling system of 'Ria de Vigo', NW Spain. FEMS Microbiol Ecol 70:493–505
3. Alonso-Sáez L, Díaz-Pérez L, Morán XAG (2015) The hidden seasonality of the rare biosphere in coastal marine bacterioplankton. Environ Microbiol 17:3766–3780
4. Alonso-Saez L, Gasol JM (2007) Seasonal variations in the contributions of different bacterial groups to the uptake of low-molecular-weight compounds in northwestern Mediterranean coastal waters. Appl Environ Microbiol 73:3528–3535
5. Álvarez-Salgado XA, Figueiras F, Fernández-Reiriz MJ, Labarta U, Peteiro L, Piedracoba S (2011) Control of lipophilic shellfish poisoning outbreaks by seasonal upwelling and continental runoff. Harmful Algae 10:121–129
6. Álvarez-Salgado XA, Figueiras F, Pérez FF, Groom S, Nogueira E, Borges AV et al (2003) The Portugal coastal counter current off NW Spain: new insights on its biogeochemical variability. Prog Oceanogr 56:281–321
7. Ambar I, & Fiúza A (1994) Some features of the Portugal current system: a poleward slope undercurrent, an upwelling-related summer southward flow and an autumn–winter poleward coastal surface current. 286-287
8. Anderson MJ, Gorley RN, Clarke KR (2008) PERMANOVA+ for PRIMER: guide to software and statistical methods. PRIMER-E, Plymouth 214 pp
9. Anderson MJ (2006) Distance-based tests for homogeneity of multivariate dispersions. Biometrics 62:245–253
10. Anderson MJ (2001) A new method for non-parametric multivariate analysis of variance. Austral Ecol 26:32–46
11. Andersson AF, Riemann L, Bertilsson S (2010) Pyrosequencing reveals contrasting seasonal dynamics of taxa within Baltic Sea bacterioplankton communities. ISME J 4:171–181
12. Arrieta JM, Weinbauer MG, Lute C, Herndl GJ (2004) Response of bacterioplankton to iron fertilization in the Southern Ocean. Limnol Oceanogr 49:799–808
13. Bano N, Hollibaugh JT (2002) Phylogenetic composition of bacterioplankton assemblages from the Arctic Ocean. Appl Environ Microbiol 68:505–518
14. Barton ED (1998) Eastern boundary of the North Atlantic: northwest Africa and Iberia. Sea 11:633–657
15. Battin TJ, Kaplan LA, Findlay S, Hopkinson CS, Marti E, Packman AI et al (2008) Biophysical controls on organic carbon fluxes in fluvial networks. Nat Geosci 1:95–100
16. Bent SJ, Forney LJ (2008) The tragedy of the uncommon: understanding limitations in the analysis of microbial diversity. ISME J 2:689–695
17. Bode A, Varela M (1998) Primary production and phytoplankton in three Galician Rias Altas (NW Spain): seasonal and spatial variability. Sci Mar 62:319–330
18. Bode A, Estévez MG, Varela M, Vilar JA (2015) Annual trend patterns of phytoplankton species abundance belie homogeneous taxonomical group responses to climate in the NE Atlantic upwelling. Mar Environ Res 110:81–91
19. Brown MV, Fuhrman JA (2005) Marine bacterial microdiversity as revealed by internal transcribed spacer analysis. Aquat Microb Ecol 41:15–23
20. Brown MV, Schwalbach MS, Hewson I, Fuhrman JA (2005) Coupling 16S-ITS rDNA clone libraries and automated ribosomal intergenic spacer analysis to show marine microbial diversity: development and application to a time series. Environ Microbiol 7:1466–1479
21. Brown MV, Lauro FM, DeMaere MZ, Muir L, Wilkins D, Thomas T. et al. (2012) Global biogeography of SAR11 marine bacteria. Molecular systems biology 8: 1–13
22. Calvo-Díaz A, Morán XAG (2006) Seasonal dynamics of picoplankton in shelf waters of the southern Bay of Biscay. Aquat Microb Ecol 42:159–174
23. Carlson CA, Morris R, Parsons R, Treusch AH, Giovannoni SJ, Vergin K (2009) Seasonal dynamics of SAR11 populations in the euphotic and mesopelagic zones of the northwestern Sargasso Sea. ISME J 3:283–295
24. Casas B, Varela M, Bode A (1999) Seasonal succession of phytoplankton species on the coast of A Coruña (Galicia, northwest Spain). Bol Inst Esp Oceanogr 15:413–430

25. Castro CG, Pérez F, Alvarez-Salgado X, Fraga F (2000) Coupling between the thermohaline, chemical and biological fields during two contrasting upwelling events off the NW Iberian Peninsula. Cont Shelf Res 20:189–210
26. Castro CG, Álvarez-Salgado XA, Figueiras F, Perez FF, Fraga F (1997) Transient hydrographic and chemical conditions affecting microplankton populations in the coastal transition zone of the Iberian upwelling system (NW Spain) in September 1986. J Mar Res 55:321–352
27. Castro CG, Pérez FF, Álvarez-Salgado XA, Rosón G, Ríos AF (1994) Hydrographic conditions associated with the relaxation of an upwelling event off the Galician coast (NW Spain). J Geophys Res 99:5135–5147
28. Chow CT, Sachdeva R, Cram JA, Steele JA, Needham DM, Patel A et al (2013) Temporal variability and coherence of euphotic zone bacterial communities over a decade in the Southern California Bight. ISME J 7:2259–2273
29. Clarke K, Gorley R (2006) PRIMER v6: user manual/tutorial. PRIMER-E, Plymouth 192 pp
30. Clarke K, Warwick R (2001) Change in marine communities: an approach to statistical analysis and interpretation2nd edn. PRIMER-E, Plymouth 172 pp
31. Coble PG (1996) Characterization of marine and terrestrial DOM in seawater using excitation-emission matrix spectroscopy. Mar Chem 51:325–346
32. Cram JA, Xia LC, Needham DM, Sachdeva R, Sun F, Fuhrman JA (2015b) Cross-depth analysis of marine bacterial networks suggests downward propagation of temporal changes. ISME J 9: 2573–2586
33. Dorst J, Bissett, A, Palmer AS, Brown M, Snape I, Stark JS et al. (2014) Community fingerprinting in a sequencing world. FEMS Microbiol Ecol 89: 316–330
34. Cram JA, Chow CT, Sachdeva R, Needham DM, Parada AE, Steele JA, Fuhrman JA (2015a) Seasonal and interannual variability of the marine bacterioplankton community throughout the water column over ten years. ISME J 9:563–580
35. Doval MD, López A, Madriñán M (2013) Spatio-temporal variability of inorganic and organic nutrients in five Galician rias (NW Spain). Sci Mar 77:15–24
36. Eiler A, Hayakawa DH, Church MJ, Karl DM, Rappé MS (2009) Dynamics of the SAR11 bacterioplankton lineage in relation to environmental conditions in the oligotrophic North Pacific subtropical gyre. Environ Microbiol 11:2291–2300
37. Eiler A, Hayakawa DH, Rappe MS (2011) Non-random assembly of bacterioplankton communities in the subtropical north pacific ocean. Front Microbiol 2:140
38. El-Swais H, Dunn KA, Bielawski JP, Li WK, Walsh DA (2014) Seasonal assemblages and short-lived blooms in coastal north-West Atlantic Ocean bacterioplankton. Environ Microbiol 17: 3642–3661
39. Estrada M (1984) Phytoplankton distribution and composition off the coast of Galicia (northwest of Spain). J Plankton Res 6: 417–434
40. Fisher MM, Triplett EW (1999) Automated approach for ribosomal intergenic spacer analysis of microbial diversity and its application to freshwater bacterial communities. Appl Environ Microbiol 65:4630–4636
41. Fiuza ADG (1984) Hidrologia e dinâmica das águas costeiras de Portugal. Faculdade de Ciências da Universidade de Lisboa, Lisbon
41. Fortunato CS, Herfort L, Zuber P, Baptista AM, Crump BC (2011) Spatial variability overwhelms seasonal patterns in bacterioplankton communities across a river to ocean gradient. ISME J 6:554–563
43. Fraga F (1981) Upwelling off the Galician coast, northwest Spain. Coastal Upwelling:176–182
44. Fraga F, Mouriño C, Manríquez M (1982) Las masas de agua en la costa de Galicia: junio-octubre. Resultado Expediciones Cientificas B/O Cornide 10:51–77
45. Frank AH, Garcia JA, Herndl GJ, Reinthaler T (2016) Connectivity between surface and deep waters determines prokaryotic diversity in the North Atlantic deep water. Environ Microbiol 18:2052–2063
46. Fuhrman JA (2009) Microbial community structure and its functional implications. Nature 459:193–199
47. Fuhrman JA, Cram JA, Needham DM (2015) Marine microbial community dynamics and their ecological interpretation. Nat Rev Microbiol 13:133–146
48. Fuhrman JA, Steele JA, Hewson I, Schwalbach MS, Brown MV, Green JL, Brown JH (2008) A latitudinal diversity gradient in planktonic marine bacteria. Proc Natl Acad Sci 105:7774–7778
49. Fuhrman JA, Hewson I, Schwalbach MS, Steele JA, Brown MV, Naeem S (2006) Annually reoccurring bacterial communities are predictable from ocean conditions. Proc Natl Acad Sci U S A 103: 13104–13109
50. García FC, Alonso-Sáez L, Morán XAG, López-Urrutia Á (2015) Seasonality in molecular and cytometric diversity of marine bacterioplankton: the re-shuffling of bacterial taxa by vertical mixing. Environ Microbiol 17:4133–4142
51. Ghiglione J, Larcher M, Lebaron P (2005) Spatial and temporal scales of variation in bacterioplankton community structure in the NW Mediterranean Sea. Aquat Microb Ecol 40:229–240
52. Ghiglione J, Galand PE, Pommier T, Pedrós-Alió C, Maas EW, Bakker K et al (2012) Pole-to-pole biogeography of surface and deep marine bacterial communities. Proc Natl Acad Sci 109: 17633–17638
53. Ghiglione JF, Murray AE (2012) Pronounced summer to winter differences and higher wintertime richness in coastal Antarctic marine bacterioplankton. Environ Microbiol 14:617–629
54. Gilbert JA, Field D, Swift P, Newbold L, Oliver A, Smyth T et al (2009) The seasonal structure of microbial communities in the Western English Channel. Environ Microbiol 11:3132–3139
55. Gilbert JA, Steele JA, Caporaso JG, Steinbrück L, Reeder J, Temperton B et al (2012) Defining seasonal marine microbial community dynamics. ISME J 6:298–308
56. Giovannoni SJ, Vergin KL (2012) Seasonality in ocean microbial communities. Science 335:671–676
57. Guerrero-Feijóo, E., Nieto-Cid, M., Sintes, E., Dobal-Amador, V., Hernando-Morales, V., Álvarez, M. et al. (2016) Optical properties of dissolved organic matter relate to different depth-specific patterns of archaeal and bacterial community structure in the north Atlantic ocean. FEMS Microbiol Ecol 93: 1–14
58. Gonzalez-Nuevo G, Gago J, Cabanas J (2014) Upwelling index: a powerful tool for marine research in the NW Iberian upwelling system. J Oper Oceanogr 7:47–57
59. Gürtler V, Mayall BC (1999) rDNA spacer rearrangements and concerted evolution. Microbiology 145:2–3
60. Hatosy SM, Martiny JB, Sachdeva R, Steele J, Fuhrman JA, Martiny AC (2013) Beta diversity of marine bacteria depends on temporal scale. Ecology 94:1898–1904
60. Haynes R, Barton ED (1990) A poleward flow along the Atlantic coast of the Iberian Peninsula. J Geophys Res Oceans 95:11425–11441
62. Hernando-Morales V, Ameneiro J, Teira E (2017) Water mass mixing shapes bacterial biogeography in a highly hydrodynamic region of the Southern Ocean. Environ Microbiol 19:1017–1029
63. Hewson I, Steele JA, Capone DG, Fuhrman JA (2006) Temporal and spatial scales of variation in bacterioplankton assemblages of oligotrophic surface waters. Mar Ecol Prog Ser 311:67–77
64. Kirchman D, K'nees E, Hodson R (1985) Leucine incorporation and its potential as a measure of protein synthesis by bacteria in natural aquatic systems. Appl Environ Microbiol 49: 599-607

65. Ladau J, Sharpton TJ, Finucane MM, Jospin G, Kembel SW, O'Dwyer J et al (2013) Global marine bacterial diversity peaks at high latitudes in winter. ISME J 7:1669–1677
66. Lande R, DeVries PJ, Walla TR (2000) When species accumulation curves intersect: implications for ranking diversity using small samples. Oikos 89:601–605
67. Langenheder S, Lindstrom ES, Tranvik LJ (2006) Structure and function of bacterial communities emerging from different sources under identical conditions. Appl Environ Microbiol 72:212–220
68. Lear G, Bellamy J, Case BS, Lee JE, Buckley HL (2014) Fine-scale spatial patterns in bacterial community composition and function within freshwater ponds. ISME J 8:1715–1726
69. Legendre P, Anderson MJ (1999) Distance-based redundancy analysis: testing multispecies responses in multifactorial ecological experiments. Ecol Monogr 69:1–24
70. Liebhold A, Koenig WD, Bjørnstad ON (2004) Spatial synchrony in population dynamics. Annu Rev Ecol Evol Syst:467–490
71. Lindh MV, Lefébure R, Degerman R, Lundin D, Andersson A, Pinhassi J (2015) Consequences of increased terrestrial dissolved organic matter and temperature on bacterioplankton community composition during a Baltic Sea mesocosm experiment. Ambio 44:402–412
72. Martínez-García S, Fernández E, Aranguren-Gassis M, Teira E (2009) In vivo electron transport system activity: a method to estimate respiration in natural marine microbial planktonic communities. Limnol Oceanogr Methods 7:459–469
73. Mary I, Cummings D, Biegala I, Burkill P, Archer S, Zubkov M (2006) Seasonal dynamics of bacterioplankton community structure at a coastal station in the western English Channel. Aquat Microb Ecol 42:119–126
74. Massana, R, Murray AE, Preston CM., & DeLong EF (1997) Vertical distribution and phylogenetic characterization of marine planktonic Archaea in the Santa Barbara Channel. Appl Environ Microbiol 63: 50-56
75. McArdle BH, Anderson MJ (2001) Fitting multivariate models to community data: a comment on distance-based redundancy analysis. Ecology 82:290–297
76. McClain CR, Chao S, Atkinson LP, Blanton JO, De Castillejo F (1986) Wind-driven upwelling in the vicinity of Cape Finisterre, Spain. J Geophys Res Oceans 91:8470–8486
77. Moeseneder MM, Winter C, Herndl GJ (2001) Horizontal and vertical complexity of attached and free-living bacteria of the eastern Mediterranean Sea, determined by 16S rDNA and 16S rRNA fingerprints. Limnol Oceanogr 46:95–107
78. Moran P (1953) The statistical analysis of the Canadianlynx cycle. II. Synchronization and meteorology. Aust J Zool 1:291–298 Moran2911Australian Journal of Zoology1953
79. Morán X, Estrada M, Gasol J, Pedrós-Alió C (2002) Dissolved primary production and the strength of phytoplankton–bacterioplankton coupling in contrasting marine regions. Microb Ecol 44:217–223
80. Morris RM, Vergin KL, Cho J, Rappé MS, Carlson CA, Giovannoni SJ (2005) Temporal and spatial response of bacterioplankton lineages to annual convective overturn at the Bermuda Atlantic time-series study site. Limnol Oceanogr 50: 1687–1696
81. Murray AE, Preston CM, Massana R, Taylor LT, Blakis A, Wu K, DeLong EF (1998) Seasonal and spatial variability of bacterial and archaeal assemblages in the coastal waters near Anvers Island, Antarctica. Appl Environ Microbiol 64:2585–2595
82. Needham DM, Chow CT, Cram JA, Sachdeva R, Parada A, Fuhrman JA (2013) Short-term observations of marine bacterial and viral communities: patterns, connections and resilience. ISME J 7:1274–1285
83. Needham DM, Fuhrman JA (2016) Pronounced daily succession of phytoplankton, archaea and bacteria following a spring bloom. Nat Microbiol 1:16005
81. Needham DM, Sachdeva R, Fuhrman JA (2017) Ecological dynamics and co-occurrence among marine phytoplankton, bacteria and myoviruses shows microdiversity matters. ISME J 11:1614–1629
85. Nogueira E, Pérez FF, Rıos A (1997) Seasonal patterns and long-term trends in an estuarine upwelling ecosystem (Rıa de Vigo, NW Spain). Estuar Coast Shelf Sci 44:285–300
86. Norland S (1993) The relationship between biomass and volume of bacteria. In: Kemp PF, Sherr BF, Sherr EB, Cole JJ (eds) Handboook of methods in aquatic microbial ecology. Lewis Publishers, Boca Raton, pp 303–307
87. Otero P, Ruiz-Villarreal M, Peliz Á, Cabanas JM (2010) Climatology and reconstruction of runoff time series in northwest Iberia: influence in the shelf buoyancy budget off Ría de Vigo. Sci Mar 74:247–266
88. Parsons TR, Maita Y, Lalli CM (1984) A manual of chemical and biological methods for seawater analysis. Pergamon Press, Oxford
89. Pedrós-Alió C (2012) The rare bacterial biosphere. Annu Rev Mar Sci 4:449–466
90. Perez FF, Mouriño C, Fraga F, Rios AF (1993) Displacement of water masses and remineralization rates off the Iberian Peninsula by nutrient anomalies. J Mar Res 51:869–892
91. Pommier T, Neal PR, Gasol JM, Coll M, Acinas SG, & Pedrós-Alió C (2010) Spatial patterns of bacterial richness and evenness in the NW Mediterranean Sea explored by pyrosequencing of the 16S rRNA
92. Pommier T, Canbäck B, Riemann L, Boström K, Simu K, Lundberg P et al (2007) Global patterns of diversity and community structure in marine bacterioplankton. Mol Ecol 16:867–880
91. Ramette A (2009) Quantitative community fingerprinting methods for estimating the abundance of operational taxonomic units in natural microbial communities. Appl Environ Microbiol 75:2495–2505
94. Riemann L, Middelboe M (2002) Stability of bacterial and viral community compositions in Danish coastal waters as depicted by DNA fingerprinting techniques. Aquat Microb Ecol 27:219–232
95. Riemann L, Steward GF, Azam F (2000) Dynamics of bacterial community composition and activity during a mesocosm diatom bloom. Appl Environ Microbiol 66:578–587
96. Ríos AF, Pérez FF, Fraga F (1992) Water masses in the upper and middle North Atlantic Ocean east of the Azores. Deep Sea Res A Oceanogr Res Pap 39:645–658
97. Ristova PP, Wenzhöfer F, Ramette A, Felden J, & Boetius A (2014) Spatial scales of bacterial community diversity at cold seeps (Eastern Mediterranean Sea). The ISME journal 9:1306–1318
98. Robinson C (2008) Heterotrophic bacterial respiration. Microbial Ecology of the Oceans, 2nd edn. pp 299–334
99. Rocap G, Distel DL, Waterbury JB, Chisholm SW. (2002). Resolution of Prochlorococcus and Synechococcus ecotypes by using 16S-23S ribosomal DNA internal transcribed spacer sequences. Appl Environ Microbiol 68: 1180–1191
100. Rosenberg MS, Anderson CD (2011) PASSaGE: pattern analysis, spatial statistics and geographic exegesis. Version 2. Methods Ecol Evol 2:229–232
101. Royama T (1992) Analytical population dynamics. Chapman and Hall, London
102. Ruiz-González C, Niño-García JP, Lapierre J, & del Giorgio PA (2015) The quality of organic matter shapes the functional biogeography of bacterioplankton across boreal freshwater ecosystems. Global Ecol Biogeogr
103. Salter I, Galand PE, Fagervold SK, Lebaron P, Obernosterer I, Oliver MJ et al (2014) Seasonal dynamics of active SAR11

ecotypes in the oligotrophic Northwest Mediterranean Sea. ISME J 9:347–360
104. Schauer M, Massana R, Pedros-Alio C (2000) Spatial differences in bacterioplankton composition along the Catalan coast (NW Mediterranean) assessed by molecular fingerprinting. FEMS Microbiol Ecol 33:51–59
105. Shade A, Jones SE, Caporaso JG, Handelsman J, Knight R, Fierer N, Gilbert JA (2014) Conditionally rare taxa disproportionately contribute to temporal changes in microbial diversity. MBio 5: e01371–e01314
106. Smith DC, Azam F (1992) A simple, economical method for measuring bacterial protein synthesis rates in seawater using 3H-leucine. Mar.Microb.Food Webs 6: 107-114
107. Sogin ML, Morrison HG, Huber JA, Mark Welch D, Huse SM, Neal PR et al (2006) Microbial diversity in the deep sea and the underexplored "rare biosphere". Proc Natl Acad Sci U S A 103: 12115–12120
104. Sokal RR, Rohlf FJ (1981) Biometry: the principles and practice of statistics in biological research. WH Freeman and Co., New York
109. Teira E, Hernando-Morales V, Fernández A, Martínez-García S, Álvarez-Salgado XA, Bode A, Varela M (2015) Local differences in phytoplankton-bacterioplankton coupling in the coastal upwelling off Galicia (NW Spain). Mar Ecol Prog Ser 528:53–69
110. Teira E, Gasol JM, Aranguren-Gassis M, Fernández A, González J, Lekunberri I, Álvarez-Salgado XA (2008) Linkages between bacterioplankton community composition, heterotrophic carbon cycling and environmental conditions in a highly dynamic coastal ecosystem. Environ Microbiol 10:906–917
111. Teeling H, Fuchs BM, Becher D, Klockow C, Gardebrecht A, Bennke CM et al (2012) Substrate-controlled succession of marine bacterioplankton populations induced by a phytoplankton bloom. Science 336:608–611
112. Teeling H, Fuchs BM, Bennke CM, Krüger K, Chafee M, Kappelmann L et al (2016) Recurring patterns in bacterioplankton dynamics during coastal spring algae blooms. elife 5:e11888
109. Treusch AH, Vergin KL, Finlay LA, Donatz MG, Burton RM, Carlson CA, Giovannoni SJ (2009) Seasonality and vertical structure of microbial communities in an ocean gyre. ISME J 3:1148–1163
114. Valencia J, Abalde J, Bode A, Cid A, Fernández E, González N et al (2003) Variations in planktonic bacterial biomass and production and phytoplankton blooms off A Coruña (NW Spain). Sci Mar 67:143–157
115. Varela M (1992) Distribution of phytoplankton size fractions during the SARP Area Cruise (April 1987) off the Galician and Cantabrian coasts (NW Spain). Bol Inst Esp Oceanogr 8:75–85
116. Vergin KL, Beszteri B, Monier A, Thrash JC, Temperton B, Treusch AH et al (2013) High-resolution SAR11 ecotype dynamics at the Bermuda Atlantic Time-series Study site by phylogenetic placement of pyrosequences. ISME J 7:1322–1332
117. Williams PJ l B, del Giorgio PA (2005) Respiration in aquatic ecosystems: history and background. In: del Giorgio PA, Williams PJ l B (eds) Respiration in aquatic ecosystems. Oxford University Press, London, pp 1–18
118. Wooster W, Bakun A, McLain D (1976) Seasonal upwelling cycle along eastern boundary of North-Atlantic. J Mar Res 34:131–141
119. Zdanowski M, Figueiras F (1999) CFU bacterial fraction in the estuarine upwelling ecosystem of Ria de Vigo, Spain: variability in abundance and their ecophysiological description. Mar Ecol Prog Ser 182:1–15